

CHARLES UNIVERSITY

Faculty of Science

Department of Organic Chemistry

Study programme: Chemistry

Branch of study: Chemistry



Natan Sidej

**Synthesis and characterization of low-molecular Fibroblast Activation Protein
inhibitors based on (*S*)-2-oxo-2-(pyrrolidin-2-yl)acetamide**

Syntéza a charakterizace nízkomolekulárních inhibitorů fibroblastového aktivačního
proteinu na bázi (*S*)-2-oxo-2-(pyrrolidin-2-yl)acetamidu

BACHELOR'S THESIS

Supervisor: Mgr. Adéla Šimková

Prague, 2021

I hereby declare that I have carried out the work independently. I proclaim that I have cited all references and literature properly. Neither this work nor a substantial part of this work were submitted elsewhere with the intention of obtaining an academic degree.

Prohlašuji, že jsem závěrečnou práci zpracoval samostatně a že jsem uvedl všechny použité informační zdroje a literaturu. Tato práce ani její podstatná část nebyla předložena k získání jiného nebo stejného akademického titulu.

Prague, 9 June 2021

Natan Sidej

Acknowledgements

First and foremost, I would like to thank my supervisor Mgr. Adéla Šimková for excellent guidance and cooperation during my past 4 years at IOCB Prague. I am also grateful to prof. RNDr. Jan Konvalinka, CSc. for giving me the opportunity to work in his team full of fantastic and inspiring people.

I would like to thank Mgr. Lenka Poštová Slavětínská, Ph. D. for the measurement of NMR spectra and assignment of signals for final compounds. I would like to thank Mgr. Tereza Ormsby, Ph. D. for the help with inhibitory potencies measurement and their evaluation. I would also like to thank all my colleagues from laboratory B2.16 for inspiring discussions, regarding organic synthesis, and for a friendly work environment.

Finally, I would like to thank my family and friends for supporting me in what I love to do.

Abstract

Fibroblast activation protein (FAP) is a serine protease which is expressed predominantly in epithelial tumor stroma and can thus be potentially used in tumor imaging and diagnosis^{1,2}. To this date, several selective and highly potent low-molecular inhibitors of FAP were developed³. However, all structure-activity relationship (SAR) studies have disregarded the region following the position of the scissile bond in the substrate. In this thesis, a total of six novel α -ketoamide FAP inhibitors were synthesized and fully characterized, in order to explore the abovementioned region. Two of the prepared inhibitors exhibit higher inhibitory potencies than the best state-of-the-art FAP inhibitors. Additionally, the effect of fluorine atoms in the C3-position of pyrrolidine on the FAP inhibitory potency and selectivity towards FAP over its homologs was examined. For this purpose, a lead-hit α -ketoamide inhibitor from a broader SAR study conducted in the Konvalinka lab at IOCB Prague was used.

Keywords: Fibroblast activation protein (FAP), protease inhibitors, serine protease, peptidomimetics, peptide chemistry, tumor visualization.

Abstrakt

Fibroblastový aktivační protein (FAP) je serinová proteasa, která je převážně exprimována ve stromatu epiteliálních nádorů^{1,2}, díky čemuž se nabízí její potenciální využití v diagnostice a zobrazování tumorů. V dnešní době existuje několik nízkomolekulárních, vysoce účinných a selektivních inhibitorů FAP. Žádná ze strukturně-aktivitních (SAR) studií se ale nezabývala oblastí, která následuje za vazbou, kterou FAP u substrátu štěpí. V rámci této práce bylo za účelem prozkoumání tohoto regionu připraveno a plně charakterizováno šest nových, α -ketoamidových inhibitorů FAP. Dva z nich vykazují silnější inhibiční schopnosti než doposud nejlepší publikovaný inhibitor FAP. V rámci práce byl také prozkoumán vliv substituce pyrrolidinového kruhu atomy fluoru na inhibiční schopnosti a selektivitu připravených inhibitorů. K tomuto účelu byl využit dosavadní nejlepší α -ketoamidový inhibitor FAP, který byl objeven v rámci širší SAR studie v laboratoři prof. Konvalinky na ÚOCHB AV ČR.

Klíčová slova: Fibroblastový aktivační protein (FAP), inhibitory proteas, serinová proteasa, peptidomimetika, chemie peptidů, vizualizace tumorů.

Abbreviations and Symbols

α_2 AP	α_2 -antiplasmin
Ac	acetyl
Ala	alanine
APCE	antiplasmin-cleaving enzyme
APT	attached proton test
Asp	aspartic acid
Bn	benzyl
Boc	<i>tert</i> -butyloxycarbonyl
boroPro	prolineboronic acid
Cbz	benzyloxycarbonyl
CMK	chloromethyl ketone
COSY	correlated spectroscopy
DCC	dicyclohexylcarbodiimide
DCM	dichloromethane
DCU	dicyclohexylurea
DIBAL-H	diisobutylaluminium hydride
DIPEA	<i>N,N</i> -diisopropylethylamine
DMAP	4-dimethylaminopyridine
DMF	<i>N,N</i> -dimethylformamide
DMP	Dess-Martin periodinane
DMSO	dimethyl sulfoxide
DP	dipeptidylpeptidase
DPPIV	dipeptidyl peptidase IV

DPP8	dipeptidyl peptidase 8
DPP9	dipeptidyl peptidase 9
EDC	1-ethyl-3-(3-dimethylaminopropyl)carbodiimide
EP	endopeptidase
EtOAc	ethyl acetate
EtOH	ethanol
EWG	electron-withdrawing group
FAP	fibroblast activation protein α
Gly	glycine
HATU	1-[bis(dimethylamino)methylene]-1 <i>H</i> -1,2,3-triazolo[4,5- <i>b</i>]pyridinium 3-oxide hexafluorophosphate
His	histidine
HMBC	heteronuclear multiple bond correlation
HPLC	high performance liquid chromatography
HRMS	high resolution mass spectrometry
HSAB	hard and soft acids and bases
HSQC	heteronuclear single quantum correlation
CH	cyclohexane
IBX	2-iodoxybenzoic acid
IC ₅₀	half-maximal inhibitory concentration
IPF	idiopathic pulmonary fibrosis
K_i	inhibitor constant
MCR	multicomponent reaction
Me	methyl
MeCN	acetonitrile

MeOH	methanol
NHS	<i>N</i> -hydroxysuccinimide
NMR	nuclear magnetic resonance
NOESY	nuclear Overhauser effect spectroscopy
PADAM	Passerini reaction-amine deprotection-acyl migration
PREP	prolyl endopeptidase
R_f	retention factor
R_t	retention time
RT	room temperature
SAR	structure-activity relationship
Ser	serine
SI	selectivity index
TEA	triethylamine
TFA	trifluoroacetic acid
THF	tetrahydrofuran
TLC	thin-layer chromatography
Ts	toluenesulfonyl
TSTU	<i>N,N,N',N'</i> -tetramethyl- <i>O</i> -(<i>N</i> -succinimidyl)uronium tetrafluoroborate
UPLC/MS	ultra-high performance liquid chromatography/mass spectrometry
Val	valine
XRD	X-ray diffraction

Table of Contents

1.	Introduction.....	10
1.1.	Fibroblast Activation Protein	10
1.1.1.	History	10
1.1.2.	Expression Patterns	10
1.1.3.	FAP Structure and its Homologs	11
1.1.4.	Enzymatic Activity and Substrate Specificity of FAP	13
1.2.	Peptidomimetic Inhibitors of Serine Proteases	15
1.2.1.	What Are Peptidomimetic Inhibitors?	15
1.2.2.	Peptidolytic Mechanism of Serine Proteases.....	15
1.2.3.	Inhibitor Warheads	16
1.2.4.	Synthetic Approaches to Peptidomimetics	19
1.2.5.	Peptide Coupling Reagents.....	20
1.2.5.1.	Carbodiimides	21
1.2.5.2.	Uronium Salt Reagents	22
1.2.6.	Multicomponent Reactions	24
1.2.6.1.	The Passerini Reaction.....	25
1.3.	FAP Inhibitors.....	28
2.	Aims of the Presented Thesis.....	31
3.	Results and Discussion	33
3.1.	Inhibitor Synthesis	33
3.2.	Evaluation of the Synthesis.....	38
3.2.1.	EDC Esterification Optimalization.....	38
3.2.2.	<i>N</i> -Boc-4,4-difluoro-L-prolinal Synthesis Optimalization.....	40
3.3.	Inhibitory Potencies of Target Compounds	41
4.	Summary and Conclusion.....	44
5.	Experimental Section.....	45

5.1. Chemicals, Materials and Equipment	45
5.2. Synthesis and Characterization of Compounds.....	46
5.3. Measurement of Inhibitory Potencies	70
6. References.....	71

1 Introduction

1.1 Fibroblast Activation Protein

1.1.1 History

Fibroblast activation protein α (FAP; EC 3.4.21.B28), also known as seprase, prolyl endopeptidase FAP or antiplasmin-cleaving enzyme (APCE), is a serine protease, discovered and identified by multiple research groups independently. Rettig *et al.* identified FAP in the late 1980's through immunochemical methods as a cell surface glycoprotein expressed in activated, proliferating fibroblasts and in malignant tissues, such as colorectal, breast, bladder, or lung carcinomas. FAP was detected as a F19 monoclonal antibody antigen which gave rise to its initial name "F19 antigen"^{1,2}.

Chen *et al.* studied FAP in 1990 under the name "seprase" as a membrane-bound protease with a collagenolytic activity. The invasive spreading of malignant cancer cells requires cleavage of the collagenous matrix present in connective tissues. Therefore, Chen *et al.* identified seprase as a potential specific marker for melanoma cells⁴. 7 years later, they published a prediction of structural properties based on a deduced amino acid sequence, described its high degree of sequence homology with an already known serine protease, dipeptidyl peptidase IV (DPPIV), and proposed, that seprase and FAP are encoded by the same gene⁵.

Finally, in 2004, Lee *et al.* have identified FAP under the name "antiplasmin-cleaving enzyme" (APCE) during their research on human α_2 -antiplasmin (α_2 AP). α_2 AP is a major inhibitor of plasmin (the enzyme responsible for fibrin digestion in blood clots) and is present in human plasma in two different forms that vary in their plasmin inhibition potencies. Lee *et al.* found that APCE promotes the transformation of α_2 AP into its more potent form⁶. Later on, they have determined that APCE is, in fact, a soluble form of FAP, present in human plasma⁷.

1.1.2 Expression Patterns

Under physiological conditions, most of the normal, healthy adult tissues show little to no detectable FAP expression levels. However, there are a few exceptions to this fact. One of them is the abovementioned soluble form of FAP, which is present in blood plasma in concentrations around 100 ng/mL (as of now, the source of plasmatic FAP is unknown)⁸.

Besides its circulating plasmatic form, FAP is also expressed in Langerhans islets⁹, bone marrow mesenchymal stem cells¹⁰ or human placenta¹¹.

An increased level of FAP expression is associated with a number of conditions that involve various tissue remodeling conditions, such as the formation of scar tissue during skin wound healing². Upregulation of FAP expression is also observed during various liver diseases, such as cirrhosis¹², liver fibrosis associated with hepatitis C¹³ or alcoholic liver disease¹⁴ (the activity of circulating plasmatic FAP was almost doubled in patients with alcoholic liver cirrhosis). On the contrary, FAP is undetectable in healthy human liver tissue.

Another example of an instance associated with increased FAP expression is idiopathic pulmonary fibrosis¹⁵ (IPF), a disease, in which the patient's lung tissue grows progressively thicker and stiffer due to scar formation. Yet again, FAP is undetectable in healthy lung tissue by immunochemical means. This further supports the trend of FAP expression in non-malignant, pathogenic tissues.

As was firstly reported by Rettig *et al.*, expression of FAP is highly upregulated in various malignant cancer cell lines. It was also shown that FAP is associated with the tumor stroma and is predominantly present in activated fibroblasts^{2,16} (which gave rise to its name, "fibroblast activation protein"). Further studies have shown that FAP might be present in other components of the tumor environment, namely in endothelial cells¹⁷ (cells on the inner surface of blood vessels that form the vessel-tissue interface) or osteoclasts¹⁸ (large, polynuclear cells responsible for the breakdown of bone tissue).

1.1.3 FAP Structure and its Homologs

FAP is a type II (single-pass with an intracellular *N*-terminus) transmembrane protease which is catalytically active only as a 170 kDa homodimer (Figure 1). Its amino acid sequence consists of a short, 6 amino acid intracellular tail, followed by a 20 amino acid transmembrane segment and a large, 734 amino acid extracellular domain, which contains the enzyme active site⁵. The plasmatic form of FAP lacks the intracellular and transmembrane segments⁷.



Figure 1 – Ribbon diagram of the FAP homodimer^{19,20}. Image from the RCSB PDB (available online at rcsb.org), Protein Data Bank ID 1Z68.

FAP belongs to the S9B peptidase subfamily (MEROPS database^{a,20}), together with its closest homolog, dipeptidyl peptidase IV (DPPIV, EC 3.4.14.5). DPPIV is the closest known homolog of FAP, having a 52% sequence identity. This peptidase, which cleaves dipeptides from its substrate's *N*-termini after a proline or alanine amino acid residue, is expressed in a broad scope of tissues and is involved in various physiological processes. For instance, DPPIV plays a key role in glucose homeostasis and its inhibition proved to be a tool for insulin secretion upregulation in patients diagnosed with type 2 diabetes mellitus. On the other hand, DPPIV is also involved in the activation, maturation, and stimulation of T cells. Therefore, the inhibition of DPPIV could resemble a double-edged blade – diabetic patients undergoing a long-term therapeutic DPPIV inhibition showed evidence of adverse immunological effects²¹. Other notable FAP homologs from the S9B subfamily are dipeptidyl peptidase 8 and 9 (DPP8 and DPP9, respectively).

Prolyl endopeptidase (PREP, EC 3.4.21.26) is a phylogenetically related FAP homolog from the S9A peptidase subfamily. It is mainly present as a soluble, cytosolic protease²², but its membrane-bound form was also found and characterized²³. PREP is strongly expressed in the human brain and is associated with aging and various neurodegenerative processes, although it is still speculated whether its proteolytic activity is the real cause of such effects²².

^a **MEROPS database** – An online database and information resource for peptidases and their protein-based inhibitors. MEROPS assigns proteases into Families, Subfamilies and Clans, based on their amino acid sequence similarities. Each peptidase is also given a unique identifier, e.g. S09.007 for FAP.

1.1.4 Enzymatic Activity and Substrate Specificity of FAP

For descriptive purposes, a conventional nomenclature developed by Schechter & Berger in 1967²⁴, was employed in this thesis. This system is commonly used to report amino acid residue sequences in protease substrates and inhibitors.

Figure 2 illustrates the basic principles. Amino acid residues are counted from the cleaved bond towards the peptide termini and are labeled with the letter P, followed by an integer. For the *N*-terminal part of the peptide, labels P1, P2, P3 etc. are used. For *C*-terminal amino acids, an apostrophe is added (P1', P2', P3'; pronounced as “P1 prime”, “P2 prime” etc.). For the corresponding active site subsites, the letter S is used.

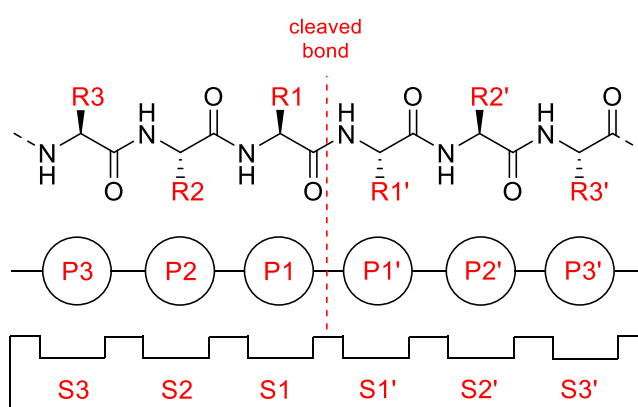


Figure 2 – Schechter & Berger nomenclature for amino acid sequences in protease substrates and inhibitors.

FAP is a unique serine protease that possesses both dipeptidyl peptidase (DP) activity and endopeptidase (EP) activity. Its DP activity, similar to DPPIV and other homologs from the S9B subfamily, consists of dipeptide cleavage from the substrate's *N*-terminus after a proline residue in position P1. A screening performed by Edosada *et al.* against a library of dipeptides with proline in P1 position and various amino acids in position P2 showed, that FAP preferentially cleaves substrates with isoleucine, arginine, and proline residues in position P2²⁵ while DPPIV does not show a marginal preference for any specific amino acids in position P2.

Contrary to the DP activity, the EP activity of FAP shows an absolute structural requirement for a glycine-proline sequence in positions P2 and P1²⁶. This is not true for PREP, the endopeptidase homolog of FAP from the S9A family – PREP readily hydrolyzes substrates bearing any L-configured amino acid in position P2, except proline²⁷. A notable mention

is the substitution of glycine in position P1 with D-alanine, which increases specificity towards FAP over PREP. However, the P1 glycine replacement also significantly decreases the affinity towards FAP's active site²⁸. Another difference in FAP and PREP substrate specificities is related to the post-proline amino acid in position P1'. A comparative study of both enzymes was carried out against a combinatorial library of P1, P1' and P2' varied peptides. The results indicate the inability of PREP to accommodate more polar amino acid residues after the scissile bond. On the other hand, FAP was able to cleave substrates with virtually any amino acid except proline in position P1'²⁹.

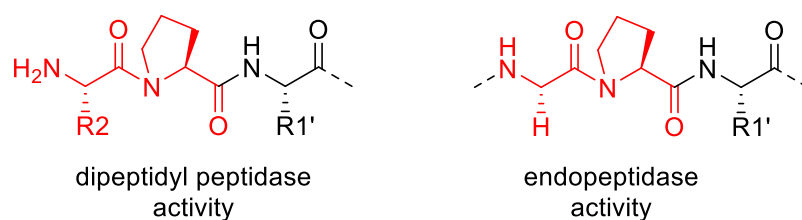


Figure 3 – Dipeptidyl peptidase and endopeptidase activities of FAP. The motif responsible for structural recognition is depicted in red.

1.2 Peptidomimetic Inhibitors of Serine Proteases

1.2.1 What Are Peptidomimetic Inhibitors?

Peptidomimetic inhibitors are compounds that are structurally designed to mimic peptides - natural substrates of peptidolytic enzymes. Their structures are usually based on an oligopeptide scaffold, which is decorated with various functional groups and substituents that ensure an optimal fit into the active site cavity. The scaffolds of peptidomimetic inhibitors are typically derived from amino acid sequences of substrates that are proven to be readily hydrolyzed by the target protease.

The main difference between a substrate and a corresponding peptidomimetic inhibitor lies in the replacement of the scissile bond by a “warhead” – a reactive group capable of interactions with the key functional groups in the protease’s active site in a similar manner as the scissile bond. Contrary to the cleaved peptide bond, the warhead does not undergo catalytical hydrolysis and therefore remains bound to the active site, rendering the protease inactive.

1.2.2 Peptidolytic Mechanism of Serine Proteases

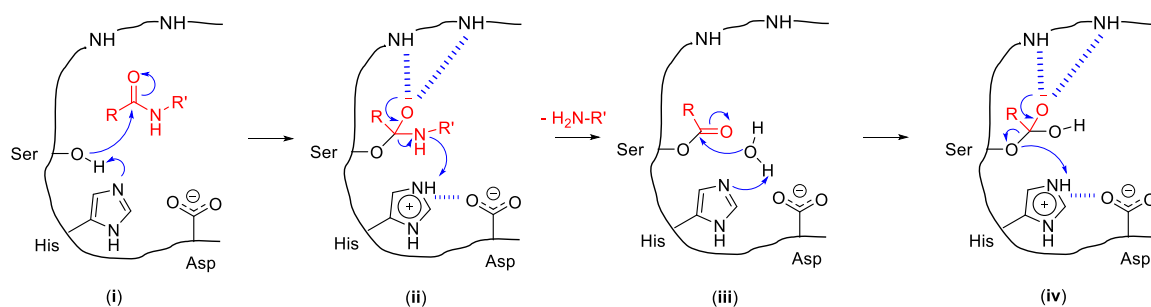
Almost a third of all known proteases in various organisms fall into the category of serine proteases, as their mechanism of peptide bond hydrolysis revolves around a nucleophilic serine hydroxyl group that plays a pivotal role during substrate cleavage.

Serine proteases are distinguished as a class of enzymes whose catalytic triad (the three amino acids responsible for an enzyme’s catalytic functionality) is comprised of serine, histidine, and aspartate residues. These amino acids cooperate to ensure hydrolysis of the scissile bond.

Scheme 1 illustrates the generally accepted mechanism of enzymatic hydrolysis, which starts with the binding of the substrate into the active site. The imidazole group of the catalytic histidine acts as a base and deprotonates the serine hydroxyl group, which then performs a nucleophilic attack on the carbon atom of the peptide bond’s carbonyl group (i). This results in the formation of a tetrahedral oxyanion intermediate, which is stabilized by the protease’s peptide backbone NH groups. Simultaneously, the formed imidazolium cation is stabilized by the catalytical triad aspartate’s negatively charged carboxylate. During the next step, the tetrahedral intermediate collapses and the scissile bond is broken, as its NH group

is protonated by the imidazolium cation and therefore becomes a suitable leaving group. This results in the formation of an acyl-serine intermediate **(ii)**.

The active site recovery is achieved *via* hydrolysis of the acyl intermediate. The imidazole deprotonates a water molecule, forming a hydroxide anion, which then performs a nucleophilic attack on the carbonyl group **(iii)**. The formed tetrahedral intermediate then collapses, expelling the catalytic serine and a carboxylic acid product and restoring the active site into its original state **(iv)**³⁰.



Scheme 1 – A general mechanism of peptide bond hydrolysis by serine proteases. The substrate is depicted in red.

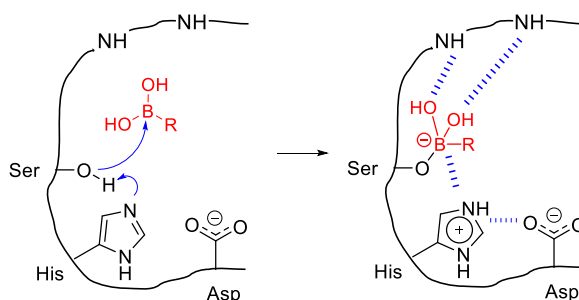
1.2.3 Inhibitor Warheads

As was previously stated, serine protease inhibition is achieved *via* replacement of the scissile bond with a warhead. There are many functional groups that can act as serine protease inhibitor warheads either *via* irreversible (e.g., alkylation, acylation, sulfonylation, phosphorylation of the catalytic amino acid residues) or reversible (structural mimicking of intermediates depicted in Scheme 1) mechanisms of inhibition.

In this thesis, the mechanism of inhibition will be illustrated only for warheads that were used in published studies on the development and optimization of FAP inhibitors. Among those are boronic acid, chloromethyl ketone, nitrile and α -ketoamide warheads.

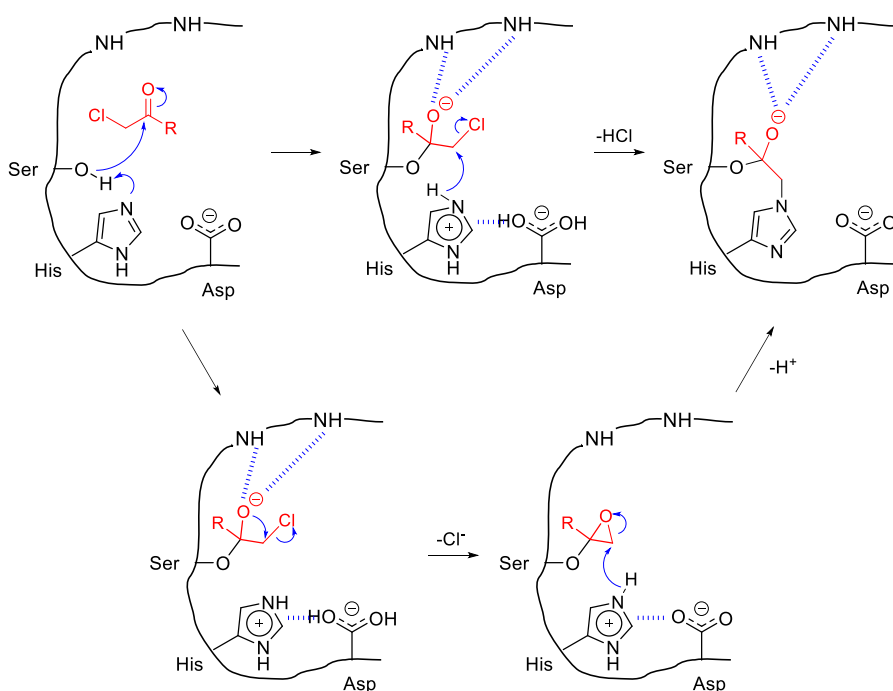
Boronic acid peptidomimetics are covalent and reversible inhibitors of serine proteases. Their structural design is based on a α -aminoboronic acid moiety, which interacts with the catalytic serine hydroxyl. The electron-deficient character, further reinforced with the geminal hydroxyl groups, makes the boron atom very susceptible towards nucleophilic attack by the serine hydroxyl. It was proven by X-ray diffraction (XRD) analysis that the resulting adduct has a near-tetrahedral geometry like the oxyanion intermediate during enzymatic hydrolysis (Scheme 1, **(ii)**). The inhibitor-enzyme complex is further stabilized

by multiple hydrogen bonds between the boronate moiety, the catalytical histidine residue and the enzyme's peptide backbone³¹. The mechanism of inhibition is illustrated by Scheme 2.



Scheme 2 – Mechanism of serine protease inhibition by boronic acid inhibitors.

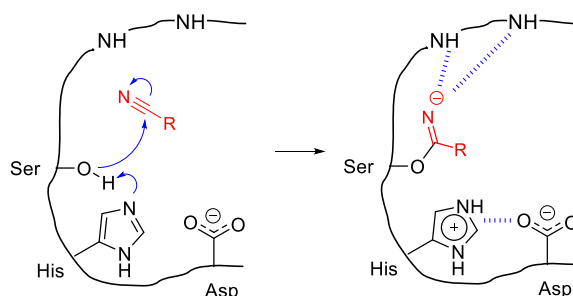
Chloromethyl ketone inhibitors belong to the category of irreversible serine protease inactivators. Firstly, they are subject to nucleophilic attack by the catalytical serine, resulting in a tetrahedral intermediate, which mimics the oxyanionic intermediate in Scheme 1. The chlorine atom then acts as a leaving group and a nucleophilic substitution by the catalytical histidine's imidazole nitrogen occurs, resulting in an irreversible cross-linkage³². Alternatively, an epoxide moiety can form, which is then opened *via* a nucleophilic attack by the histidine nitrogen³³, resulting in the same cross-linkage. The possible mechanisms of inhibition by chloromethyl ketones are shown in Scheme 3.



Scheme 3 – Mechanisms of serine protease inhibition by chloromethyl ketone inhibitors.

Later, also bromomethyl and iodomethyl ketones were studied and they showed increased reactivity and inhibitory potencies but were less stable in aqueous environments. On the contrary, fluoromethyl ketones, due to the relative unreactivity of C-F bonds, proved to be only weak and reversible inactivators of serine proteases. However, this is not the case for difluoro- and trifluoromethyl ketones, which are potent serine protease inhibitors³³.

Nitrile inhibitors are known as covalent and reversible inhibitors of cysteine and serine proteases. Their mechanism of inhibition is based on the formation of an imidate anion with the serine hydroxyl (or a thioimidate in the case of cysteine proteases), which resembles the acyl-enzyme intermediate during enzymatic hydrolysis of peptides³⁴ (Scheme 4). Initially, nitrile inhibitors were not thought of as suitable serine protease inhibitors.



Scheme 4 – Mechanism of serine protease inhibition by nitrile inhibitors.

According to Pearson's Hard and Soft Acids and Bases (HSAB) theory, the nitrile moiety is a soft electrophile that preferentially reacts with soft nucleophiles, such as the thiol group of cysteine proteases, over the typical hard nucleophiles like the serine hydroxyl groups³⁵. Thus, the interaction between nitrile inhibitors and serine proteases was not investigated for a substantial period of time. However, during the investigation of the role of DPPIV (homolog of FAP discussed in Section 1.1.3, page 11) in glucose metabolism, two potent, reversible and slow-binding nitrile inhibitors of DPPIV, Vildagliptin³⁶ and Saxagliptin³⁷ (Figure 4) were discovered. Subsequent XRD analysis of a DPPIV-Saxagliptin complex crystal revealed, that nitrile inhibitors do form the presumed covalent imidate adduct with serine proteases³⁸.

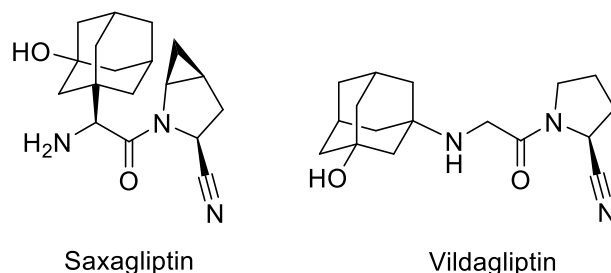
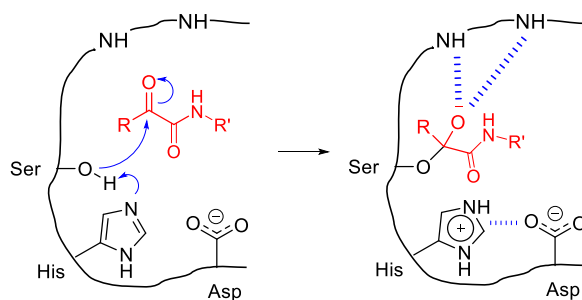


Figure 4 – Nitrile inhibitors of DPPiV Saxagliptin and Vildagliptin.

α -Ketoamides are a class of reversible covalent serine protease inhibitors that provide an enzyme-inhibitor adduct with the highest degree of similarity (among the inhibitor warheads discussed in this chapter) to the oxyanion enzyme-substrate adduct (Scheme 1). The inhibitory potency of α -ketoamides is based on the absence of a good leaving group in the enzyme-inhibitor adduct, opposed to the enzyme-substrate adduct. A general mechanism of inhibition is depicted in Scheme 5.



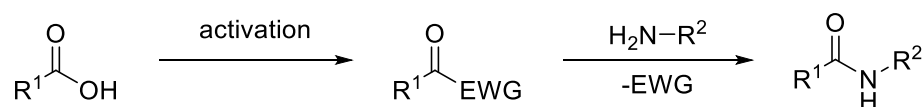
Scheme 5 – Mechanism of serine protease inhibition by α -ketoamide inhibitors.

1.2.4 Synthetic Approaches to Peptidomimetics

Peptidomimetics are compounds that are based on an oligopeptide scaffold, decorated with various moieties needed to ensure their desired functionality. There are two common synthetic approaches to such compounds. One is based on a retrosynthetic disconnection to various amino acid derivatives and their further condensation with the aid of peptide coupling reagents – compounds that facilitate the creation of a peptide bond from a carboxylic acid and an amine. The other method involves multicomponent reactions, whose general characteristic is an excellent atom economy and a suitability for syntheses of broad libraries of compounds and for structure-activity-relationship (SAR) studies. Both approaches will be further discussed in a scope that provides theoretical background and explanation for the synthetic methods used in the experimental part of this thesis.

1.2.5 Peptide Coupling Reagents

Peptide coupling reagents are compounds that enable the synthesis of amides from carboxylic acids and amines. There is a plethora of available reagent types and classes, but the main principle remains the same. The formation of an amide bond is achieved through the activation of the carboxylic acid by the introduction of an electron-withdrawing group³⁹ (EWG, Scheme 6). Among these are halides, symmetric or mixed anhydrides and active esters. All these functionalities can act as good leaving groups, which enables the formation of an amide after a nucleophilic addition of an amine to the activated carboxylic acid.



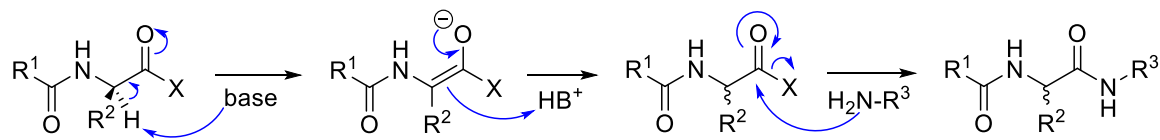
Scheme 6 – Basic principle of amide synthesis with peptide coupling reagents.

One of the notable differences between various peptide coupling reagents is the stability of the activated species. Some reagents provide stable activated compounds that can be isolated and stored for prolonged amounts of time, such as *N*-hydroxysuccinimide (NHS) esters. Other reagents provide more reactive species, which usually have only limited shelf-lives, a typical example being acyl halides or some anhydrides. The strongest peptide coupling reagents typically form unisolable, metastable active compounds that readily collapse with any suitable nucleophile.

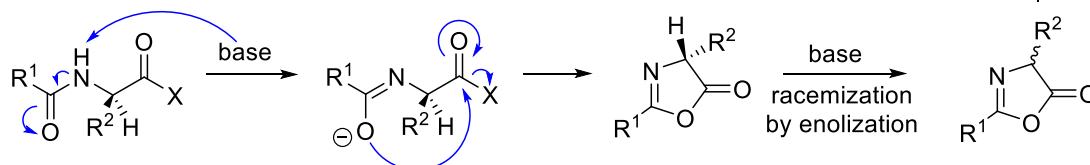
Despite the ongoing advances in peptide coupling chemistry, the use of coupling reagents still faces one major obstacle, which is racemization of chiral reactants, most often associated with carboxylic acids bearing a chiral α -carbon. During the activation process, a partial loss of chirality can occur. This is a critical problem in the synthesis of peptidomimetics because a defined absolute configuration is often essential for a proper activity of bioactive compounds.

Currently, there are two generally accepted mechanisms of racemization during peptide coupling reactions. One is the direct enolization of the carboxylic acid reactant, in which the α -proton is abstracted by a base and chirality is lost, due to the planar geometry of the arisen enolate anion. The other mechanism is based on the intramolecular oxazolone creation and its further racemization by base-catalyzed enolization⁴⁰. Both pathways are illustrated in Scheme 7.

a) enolization



b) oxazolone formation



Scheme 7 – General mechanisms of racemization during peptide coupling reactions.

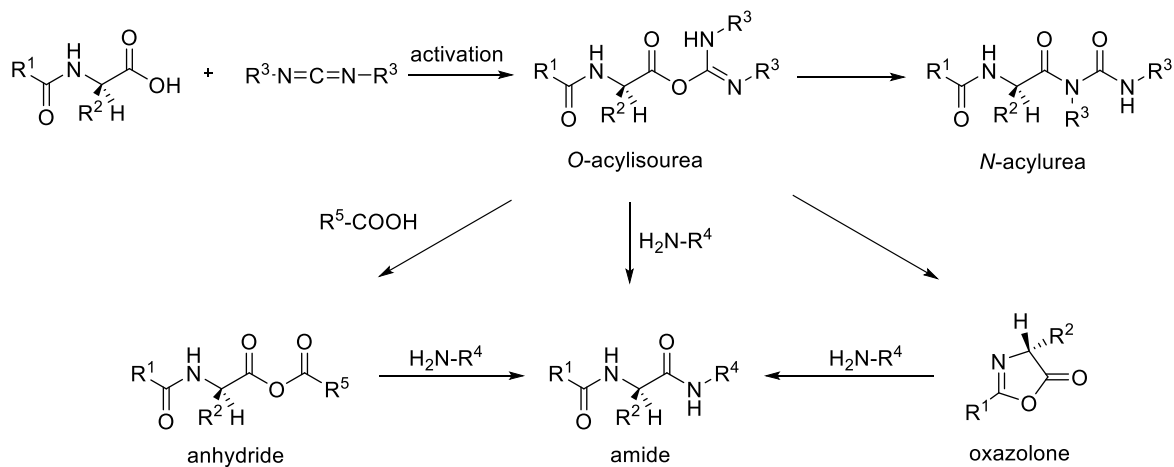
There are various methods of racemization suppression. Firstly, the use of *N*-terminal carbamate protecting groups, such as the popular *tert*-butyloxycarbonyl (Boc) and benzyloxycarbonyl (Cbz) groups, reduces the tendency of oxazolone formation^{41,42}. Secondly, the absence of electron-withdrawing groups greatly suppresses enolization. Finally, the use of bulkier tertiary amines, which are commonly used as bases in peptide coupling reactions, significantly attenuates α -proton abstraction⁴³. A great example of such base is *N,N*-diisopropylethylamine (DIPEA), a widely used staple in peptide chemistry.

The scope of peptide coupling chemistry has been summarized multiple times in thorough reviews^{39,44–46}. Carbodiimides and uronium salt reagents were the reagents of choice during the synthetic part of this thesis and will be reviewed in more detail.

1.2.5.1 Carbodiimides

Carbodiimides are among the oldest and most traditional peptide coupling reagents. Various carbodiimide reagents differ in the nitrogen substituents, which give rise to differences in chemical reactivity and properties. The mechanism of activation (Scheme 8) is based on the acid deprotonation by the carbodiimide nitrogen, followed by a nucleophilic attack by the carboxylate, which results in the formation of an *O*-acylisourea. The *O*-acylisourea is highly reactive and undergoes aminolysis to give the corresponding amide⁴⁷. Alternatively, in the presence of a carboxylic acid, an anhydride is generated, which can be then aminolyzed to the desired amide. The *O*-acylisourea can, to some extent, cyclize to an oxazolone, which is less reactive and thus prone to racemization (following the same mechanism as was shown in Scheme 7). An undesired side-reaction is the intramolecular rearrangement of the *O*-acylisourea to the corresponding *N*-acylurea. This rearrangement,

which renders the carboxylic acid unreactive, can be suppressed by various additives, typically based on a benzotriazole scaffold⁴⁸.



Scheme 8 – Carbodiimide activation of carboxylic acids and the reactivity of generated *O*-acylisourea.

Examples of carbodiimide reagents are shown in Figure 5. Dicyclohexylcarbodiimide (DCC) is the most traditional carbodiimide reagent. It produces a dicyclohexylurea (DCU) byproduct during the peptide coupling reaction, which is practically insoluble in all commonly used organic solvents, allowing an easy reaction work-up by filtration. DCU is soluble only in trifluoroacetic acid, which makes it compatible with *N*-Boc-protection based solid phase synthesis of peptides.

An exact opposite of DCC is *N*-ethyl-*N'*-(3-dimethylaminopropyl)carbodiimide (EDC), commonly supplied as a hydrochloride salt. EDC produces a urea byproduct which is soluble in water and can be therefore removed by extraction, making EDC a suitable choice for solution-based peptide coupling chemistry.

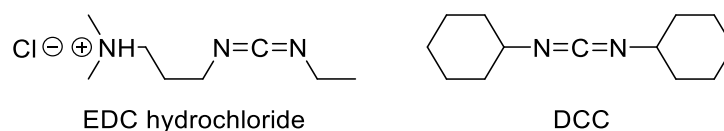


Figure 5 – Examples of carbodiimide peptide coupling reagents.

1.2.5.2 Uronium Salt Reagents

Uronium salt reagents are compounds that are based on a *N,N,N',N'*-tetrasubstituted urea scaffold (Figure 6). The urea oxygen atom carries the activating group, most commonly a *N*-hydroxysuccinimidyl, *N*-benzotriazolyl, *N*-azabenzotriazolyl moiety or some related

derivative. The proposed mechanism (Scheme 9) lies in the formation of a carboxyl uronium salt, from which the tetrasubstituted urea byproduct is then expelled and a corresponding active ester is formed⁴³. Amide formation is then achieved by its aminolysis. These active esters are usually highly unstable and cannot be isolated or stored as stock solutions for prolonged periods of time.

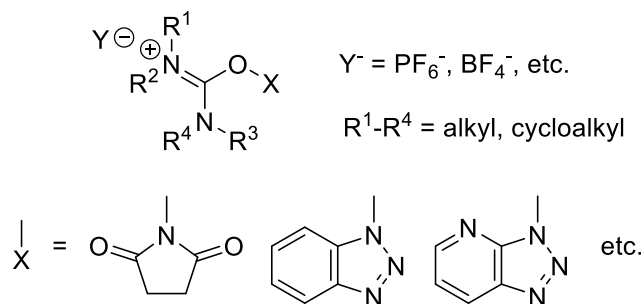
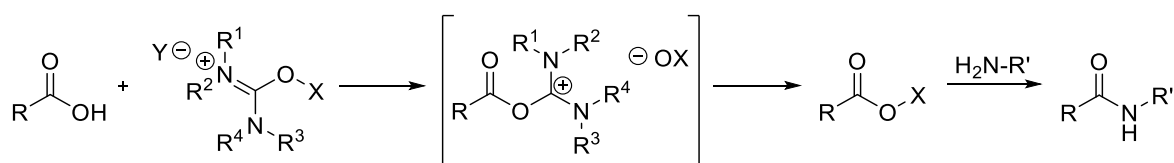


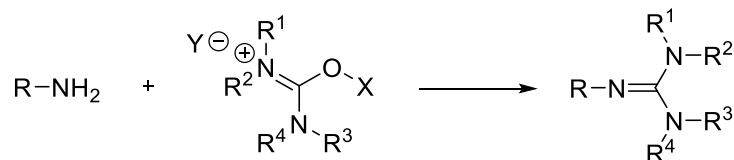
Figure 6 – A general structure of uronium salt peptide coupling reagents.



Scheme 9 – A general scheme of peptide coupling with uronium salt reagents.

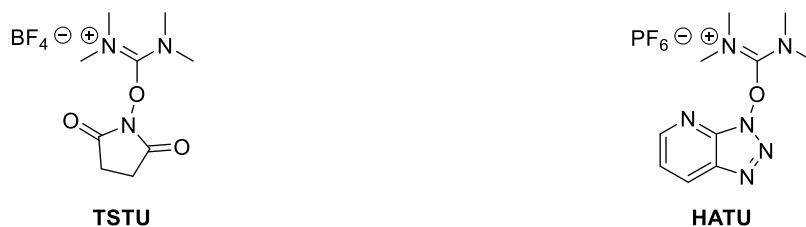
The undisputed advantage of uronium salt reagents over carbodiimides is their higher reactivity, associated with a lower degree of racemization⁴⁹. The standard coupling procedure is based on the preactivation of the carboxylic acid, forming a solution of the active ester, to which the amine is then added. On the other hand, uronium salt reagents come at a higher price and they also have a shorter shelf-life.

A weak point of uronium salt reagents is their reactivity towards amines, which results in the formation of guanidine side-products (Scheme 10), essentially destroying the amine starting material⁵⁰. The rate of this reaction is lower by several orders of magnitude, compared to the carboxylic acid activation, however, can still occur to a notable extent. For this reason, a proper preactivation of the carboxylic acid is necessary to ensure that most of the reagent will have reacted by the time the amine is added.



Scheme 10 – The side-reaction of uronium salt reagents with amines.

There is well over 70 published and studied uronium salt coupling reagents that are formed by different combinations of substituents R¹-R⁴, activating groups X and counterions Y. A review³⁹ by El-Faham and Albericio provides an in-depth summary. During the synthetic part of this thesis, two uronium salt reagents, TSTU and HATU, were employed (Figure 7). TSTU is used for the formation of NHS-esters, HATU forms more reactive, but unstable 1-hydroxy-7-azabenzotriazole active esters. HATU is also known for its low degrees of racemization during peptide coupling reactions (see ref.⁵¹).



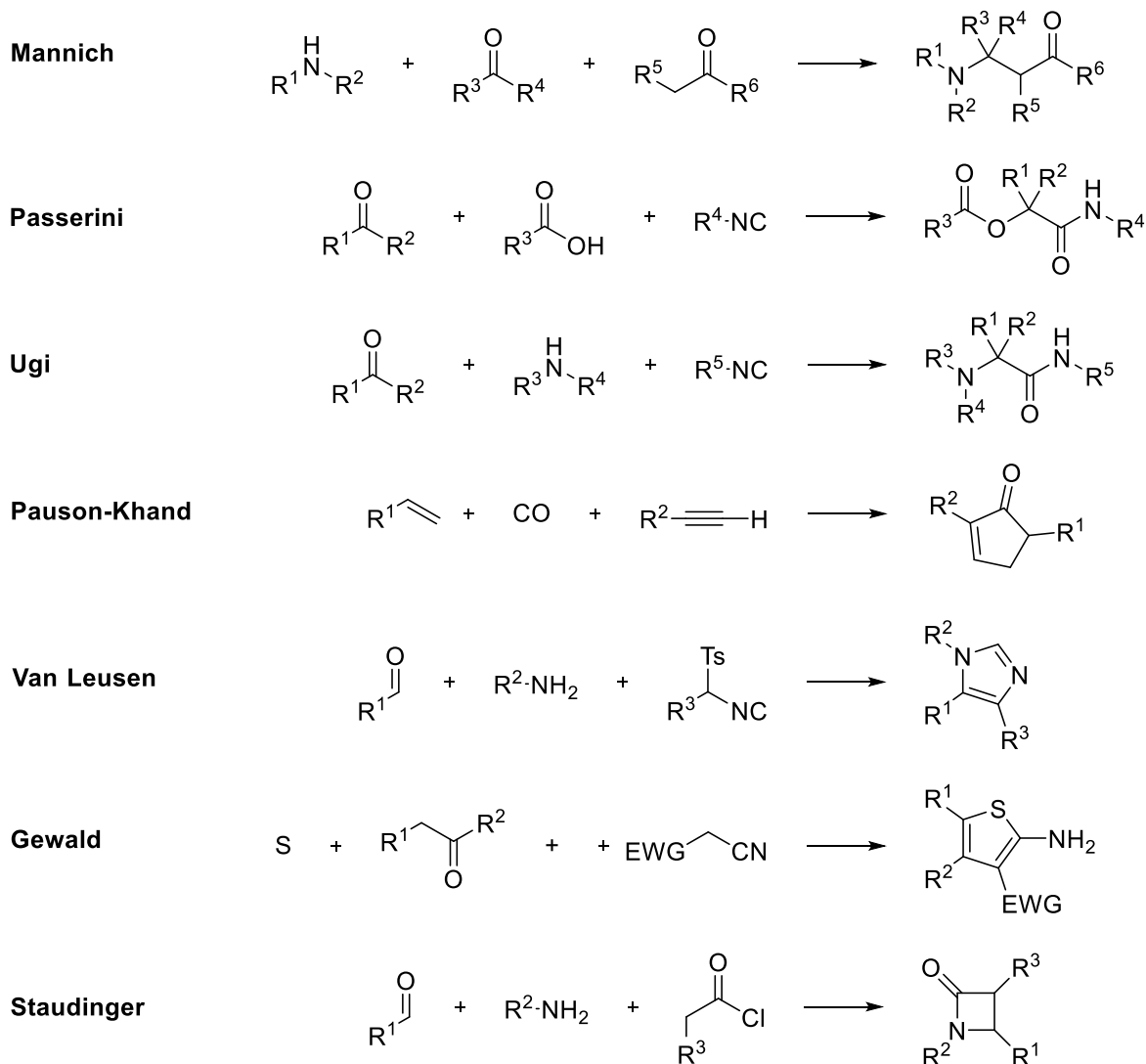
TSTU
tetrafluoroborate *N*-succinimidyl tetramethyl uronium

HATU
hexafluorophosphate azabenzotriazole tetramethyl uronium

Figure 7 – Examples of uronium salt coupling reagents, TSTU and HATU, together with the acronym explanations.

1.2.6 Multicomponent Reactions

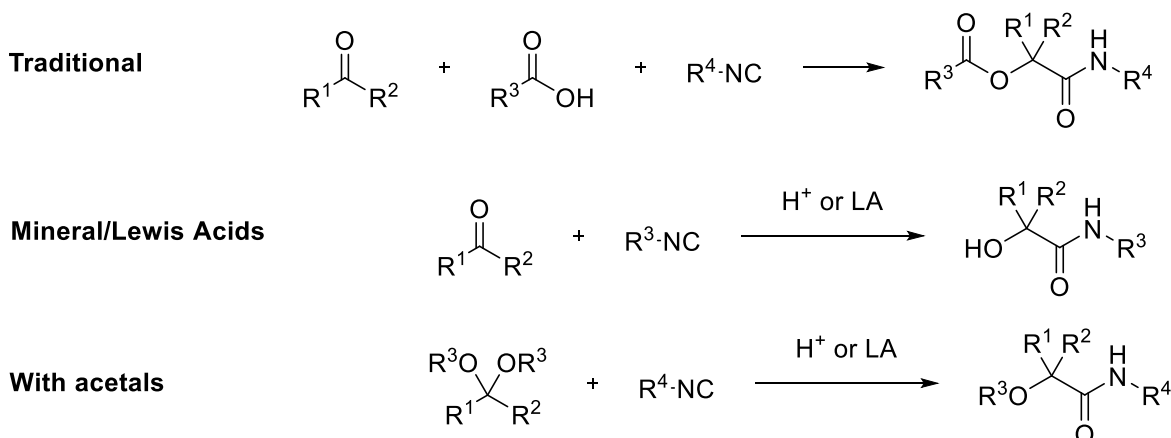
Over the past decades, an increasing interest in the research of multicomponent reactions (MCRs) has been observed. MCRs are defined as reactions that employ three or more reactants and have a good atom economy – a measure, which shows how many of the reactant atoms end up incorporated into the product's structure⁵². Not only do MCRs offer good yields, which are desired by the chemical industry, but they also provide a way of synthesizing broad libraries of compounds that can be used in structure-activity relationship studies. Today, MCRs are widely employed in the synthesis of peptidomimetic compounds (Mannich⁵³, Passerini⁵⁴, Ugi⁵⁵ reactions), cyclic and heterocyclic compounds (Pauson-Khand⁵⁶, Van Leusen⁵⁷, Gewald⁵⁸ reactions) or β -lactams (Staudinger synthesis⁵⁹). Scheme 11 illustrates these examples. During the synthetic part of this thesis, the Passerini MCR was employed to great extent and will be therefore discussed in more detail.



Scheme 11 – Examples of multicomponent name reactions.

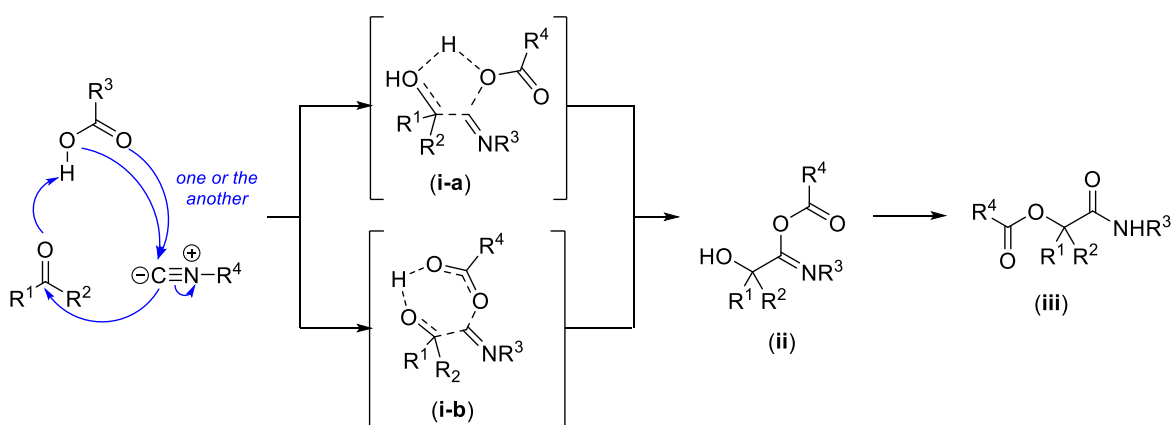
1.2.6.1 The Passerini Reaction

The Passerini reaction, discovered by Mario Passerini in 1921 at the University of Florence, is the first MCR which involves an isocyanide as one of the reactants. The classical Passerini reaction is understood as the reaction between a carboxylic acid, an aldehyde or ketone and an isocyanide, forming a α -acyloxyamide product⁵⁴. Modern takes on the Passerini reaction, based on the replacement of carboxylic acids with mineral or Lewis acids, lead to the formation of α -hydroxyamides. Replacement of the carbonyl reactant with an acetal gives rise to the formation of α -alkoxyamides⁶⁰ (Scheme 12).



Scheme 12 – Modifications of the Passerini reaction.

The generally accepted mechanism was postulated by Ivar Ugi in 1961⁶¹ and is depicted in Scheme 13. It is assumed, that the reactants first react in a concerted manner to form a cyclic transition state. The cycle can be 5-membered (**(i-a)**) or 7-membered (**(i-b)**), depending on which oxygen atom of the carboxylic acid attacks the isocyanide carbon atom. The transition state then collapses, forming the intermediate (**(ii)**), after which an *O-O* transacylation occurs, generating the final product of the reaction (**(iii)**). This mechanism is also in agreement with the observations, that the reaction rate is dependent on all three reactants⁶² (supports the concerted mechanism) and that the reaction occurs faster in non-polar solvents⁶³ (disproved a previously suggested mechanism with ionic intermediates).



Scheme 13 – The generally accepted mechanism of the Passerini reaction.

As the α -acyloxyamide Passerini reaction product is a suitable precursor towards peptidomimetic compounds, the stereochemical aspects of the reactions need to be addressed – as was previously discussed, the optical purity of peptidomimetics is essential in order to exhibit ensure their desired biochemical activities.

It has been shown that racemization is not expected to occur under the mild and neutral reaction conditions. To demonstrate this, various studies with optically pure α -aminoaldehydes as reactants were conducted. It has been shown that their configurations were retained in both the classical and Lewis acid catalyzed Passerini reactions⁶⁴⁻⁶⁷. However, not all α -substituted aldehydes were configurationally stable. For instance, α -alkylated aldehydes did show a significant degree of racemization⁶⁸.

Experimental evidence for the retention of chiral configuration in α -substituted isocyanides during Passerini reactions has been provided multiple times^{65,69,70}. However, care has to be taken in the case when the isocyanides are prepared from their corresponding formamides – it was observed that their dehydration to isocyanides with dehydrating reagents, such as phosphoryl chloride or diisopropylamine, was accompanied by significant loss of stereochemical integrity⁷¹. A suitable dehydration method which yields enantiomerically pure isocyanides is achieved by diphosgene or triphosgene^{69,70}. These compounds, however, can evolve phosgene, an extremely toxic gas, and therefore require proper handling.

Carboxylic acids with chiral α -carbons have not been reported to lose chirality during Passerini reactions⁷²⁻⁷⁴.

1.3 FAP Inhibitors

The first inhibitors of FAP were developed and published by Hu *et al.* in 2005⁷⁵. The study has resulted in the discovery of a potent FAP and DPPIV inhibitor Val-boroPro, based on a valyl-prolyl dipeptide scaffold, bearing a boronic acid warhead (Figure 8). Despite its unsatisfactory FAP/DPPIV selectivity, the compound Val-boroPro has entered early clinical trials under the name Talabostat, due to its nanomolar IC₅₀ and its anti-tumor therapeutic potential⁷⁶.

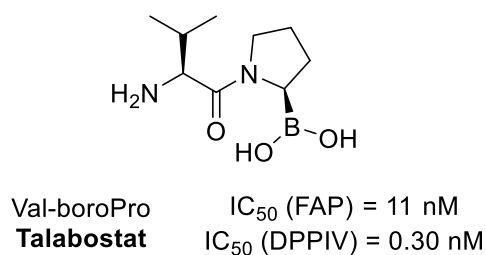


Figure 8 – Val-boroPro (Talabostat), one of the first published FAP inhibitors.

Other studies by Edosada *et al.* have focused on the improvement of FAP/DPPIV selectivity by various *N*-terminal substitutions. Their efforts have led to the development of a selective FAP inhibitor, *N*-acetyl-glycyl-prolineboronic acid (Ac-Gly-boroPro, Figure 9), which exhibited good selectivity towards FAP over its dipeptidyl peptidase homologs²⁵.

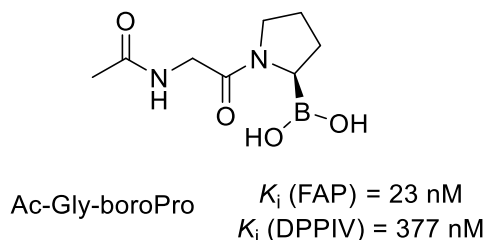


Figure 9 – A selective FAP inhibitor, Ac-Gly-boroPro. The inhibitory potencies are given in inhibitor constants, K_i , which are equal to inhibitor concentrations needed for half-maximum inhibition of the target enzyme.

Following this discovery, two analogs of Ac-Gly-boroPro with different warheads were prepared (Figure 10). The first one was an chloromethyl ketone (CMK) inhibitor, which showed mediocre FAP affinity and also inhibited the related endopeptidase PREP⁷⁷. The second derived inhibitor was equipped with a soft-electrophilic nitrile warhead. It exhibited a micromolar K_i value for FAP and a one order of magnitude lower affinity towards DPPIV⁷⁸.

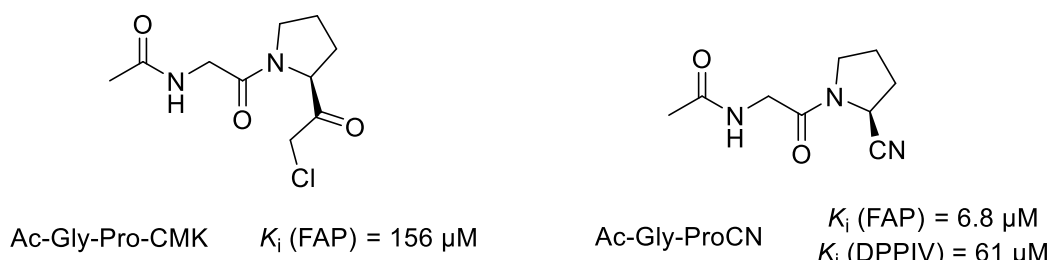


Figure 10 – Ac-Gly-Pro based inhibitors with chloromethyl ketone and nitrile warheads.

Later, Tsai *et al.* have discovered that some nitrile inhibitors that were designed to inhibit DPPIV were also inhibiting FAP (Figure 11). Therefore, they have decided to perform a SAR study targeting FAP with nitrile-based inhibitors instead of boronic acids – they assumed, that the milder electrophility of the nitrile warhead would provide better selectivity *in vivo* towards FAP over DPPIV and PREP, compared to the available boronate-based inhibitors. This gave rise to the nitrile-class of FAP inhibitors⁷⁹.

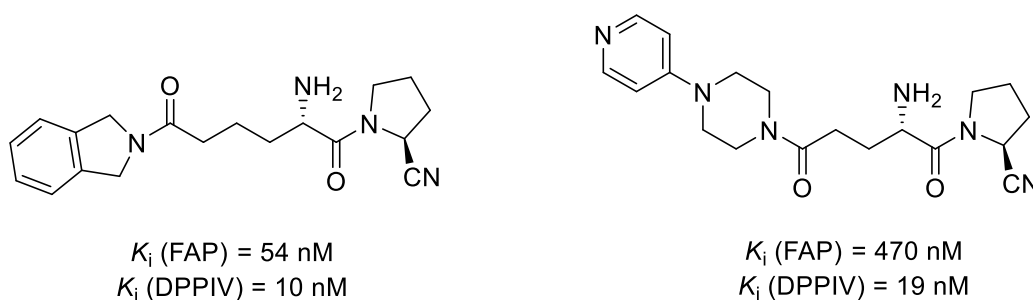


Figure 11 – DPPIV nitrile inhibitors that were found to inhibit FAP as well by Tsai *et al.*

In 2013, two additional research groups simultaneously tried to overcome the so far unsuccessful attempts on designing FAP inhibitors that have a good FAP/PREP selectivity. Jansen *et al.* have investigated the effects of different P3 substitutions on the FAP/PREP selectivity, discovering their lead nitrile inhibitor, which bears a 4-quinolinoyl moiety in P3 position⁸⁰ (Figure 12). This inhibitor is used as a reference compound in the experimental part of this thesis and will be referred to as **R1**.

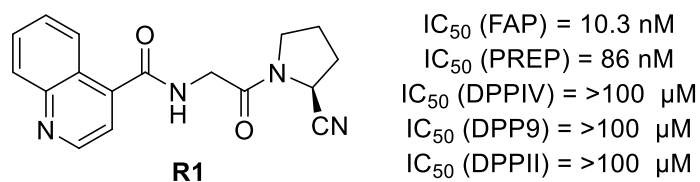
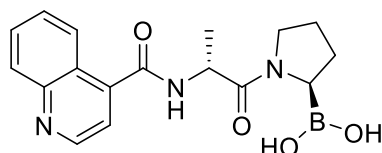


Figure 12 – A nanomolar FAP inhibitor developed by Jansen *et al.*, used as a reference compound in this thesis.

Poplawski *et al.* have found important remarks regarding the P2-position amino acid residue, using the already well known prolineboronic acid-based inhibitors. Their results indicate, that FAP is, to some extent, able to tolerate D-amino acids in position P2, whereas affinities towards PREP were absolutely compromised by these substitutions. The best results were achieved with a D-alanine residue in position P2²⁶ (Figure 13).

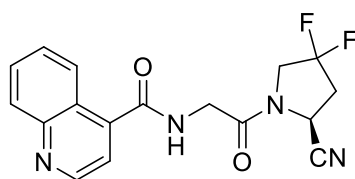


$$IC_{50} (\text{FAP}) = 6.4 \text{ nM}$$

$$IC_{50} (\text{PREP}) = 1 \text{ }\mu\text{M}$$

Figure 13 – An inhibitor with great FAP/PREP selectivity, discovered by Poplawski *et al.*

Finally, Jansen *et al.* have put all these findings together and tested a compound based on the structure of inhibitor **R1** with a D-alanine instead of glycine in position P2. Contrary to the observations by Poplawski *et al.*, the insertion of D-alanine did not lead to an increase of FAP/PREP selectivity in the case of a nitrile inhibitor. Jansen *et al.* have also tried substituting the C3 hydrogens of the **R1** inhibitor's pyrrolidine ring with fluorine atoms, which has led to the discovery of the best state-of-the-art FAP inhibitor **R2** (Figure 14). This compound displayed a low nanomolar affinity towards FAP (3.2 nM), a 562-fold lower affinity towards PREP (1.8 μM) and virtually no affinities to the DPP enzymes. Inhibitor **R2** was also tested *in vivo* in mice and was found to have high oral bioavailability and a plasma half-life, making it a promising compound for further experiments³.



R2

$$IC_{50} (\text{FAP}) = 3.2 \text{ nM}$$

$$IC_{50} (\text{PREP}) = >1.8 \text{ }\mu\text{M}$$

$$IC_{50} (\text{DPPIV}) = >100 \text{ }\mu\text{M}$$

$$IC_{50} (\text{DPP9}) = >12.5 \text{ }\mu\text{M}$$

$$IC_{50} (\text{DPP11}) = >100 \text{ }\mu\text{M}$$

Figure 14 – The best state-of-the-art FAP inhibitor, discovered by Jansen *et al.*

2 Aims of the Presented Thesis

As was illustrated in previous chapters, FAP is a serine protease with unique properties that make it a very promising platform for potential tumor diagnostics and other therapeutical applications on the field of medicinal chemistry. Over the past three decades, research of FAP has resulted in the discovery of highly optimized and potent low-molecular inhibitors, creating opportunities for further scientific work.

Up to this date, no published studies have examined the “C-terminal” region beyond the inhibitor warhead. Therefore, it is necessary to explore the effects of structural changes in positions P1’ and P2’ on the behavior of inhibitors towards FAP and its related homologs, namely DPPIV and PREP. To achieve this, a new class of α -ketoamide compounds has been designed (submitted for publication).

- 1) The main aim of this thesis is the preparation and characterization of novel α -ketoamide compounds (Figure 15). These compounds were designed to examine the influence of various substitutions in the P2’ position. Afterwards, inhibitory potencies of these compounds towards FAP will be evaluated and compared with reference inhibitors **R1** and **R2**, which will be also prepared according to literature and characterized.

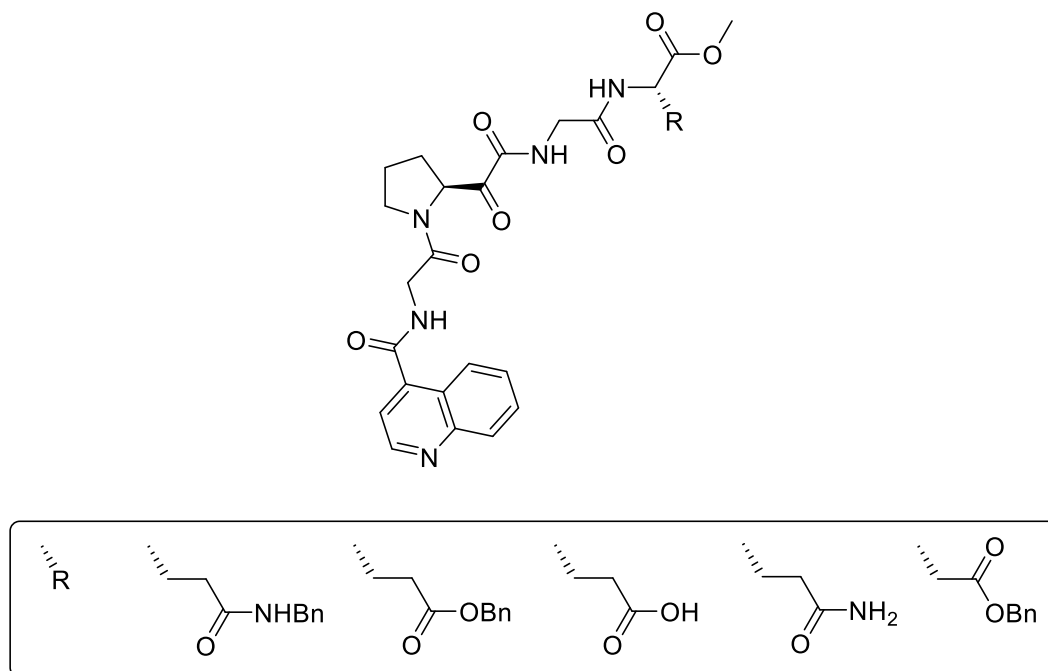


Figure 15 – Designed novel α -ketoamide compounds, whose synthesis, characterization, and biochemical evaluation is the main aim of this thesis.

2) Furthermore, the influence of the pyrrolidine C3-hydrogens substitution with fluorine atoms will be studied. A lead α -ketoamide inhibitor **R3**, discovered within this FAP project, has been chosen as a model compound for this task (Figure 16). A corresponding derivative will be prepared and characterized, in order to determine the effect of this substitution on the FAP inhibitory potency and on the FAP/PREP selectivity – according to literature, the substitution has been beneficial in both cases.

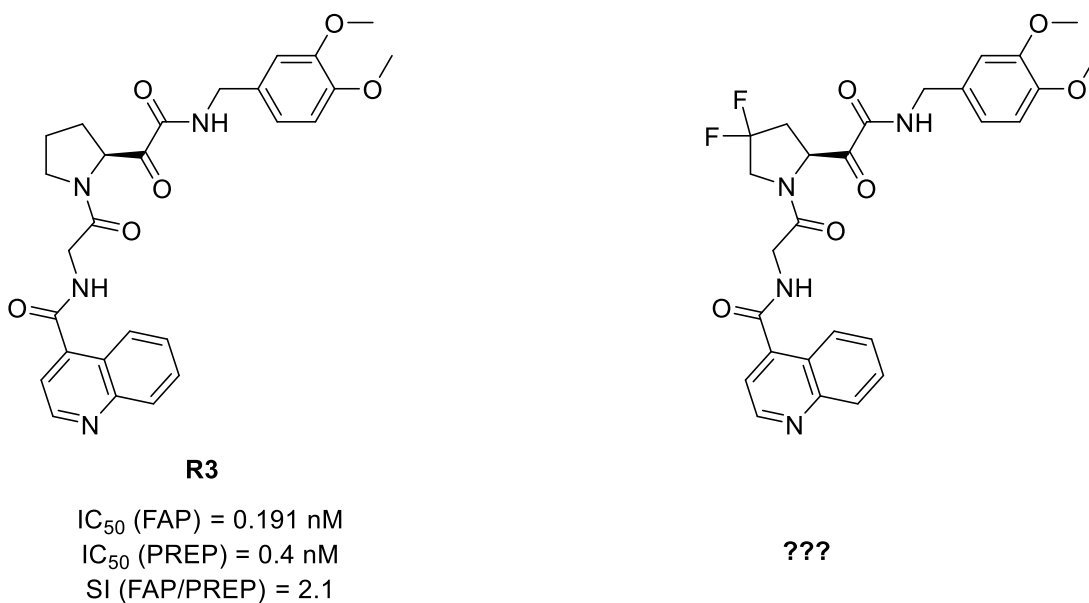


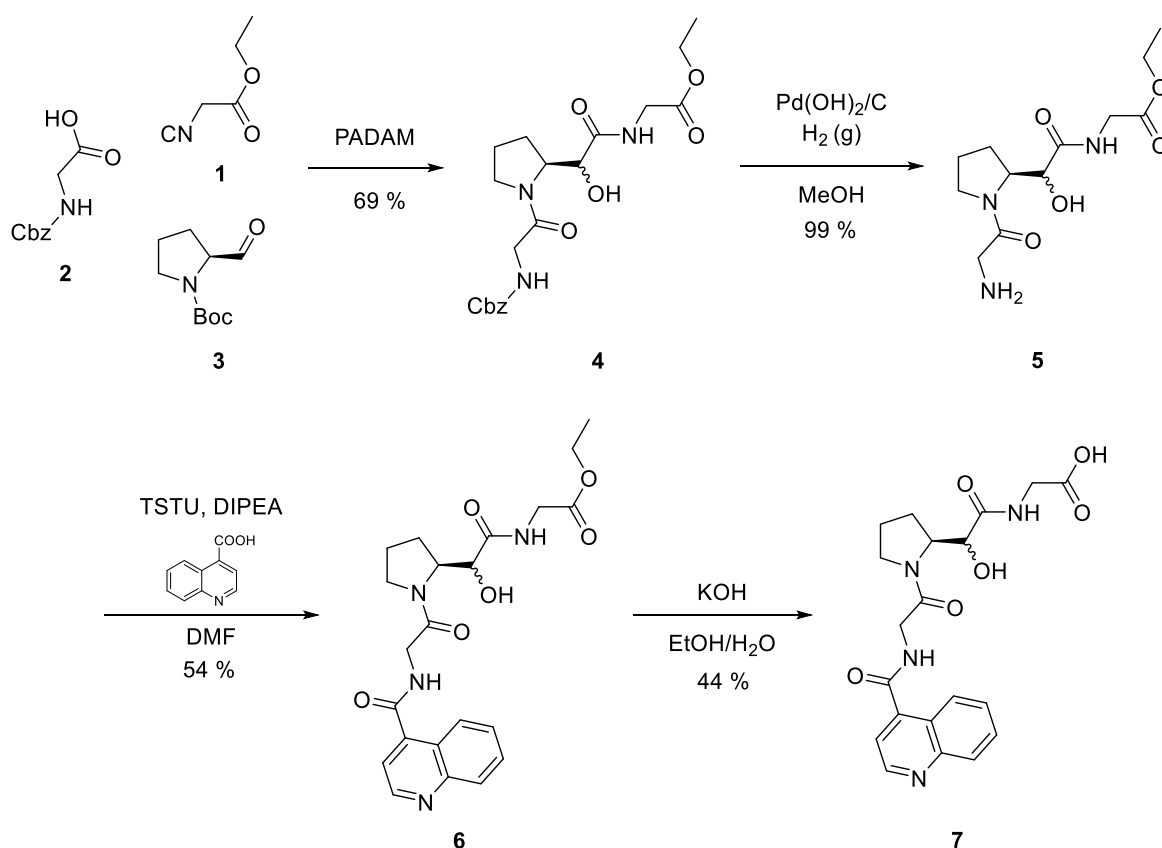
Figure 16 – The lead-hit α -ketoamide FAP inhibitor and its derivative bearing fluorine atoms in the pyrrolidine C3-position. SI (FAP/PREP) is the selectivity index, given by the ratio of IC_{50} (PREP) to IC_{50} (FAP).

3 Results and Discussion

3.1 Inhibitor Synthesis

The synthesis of target compounds was carried *via* preparation of various building blocks and their subsequential condensation, followed by a final oxidation reaction.

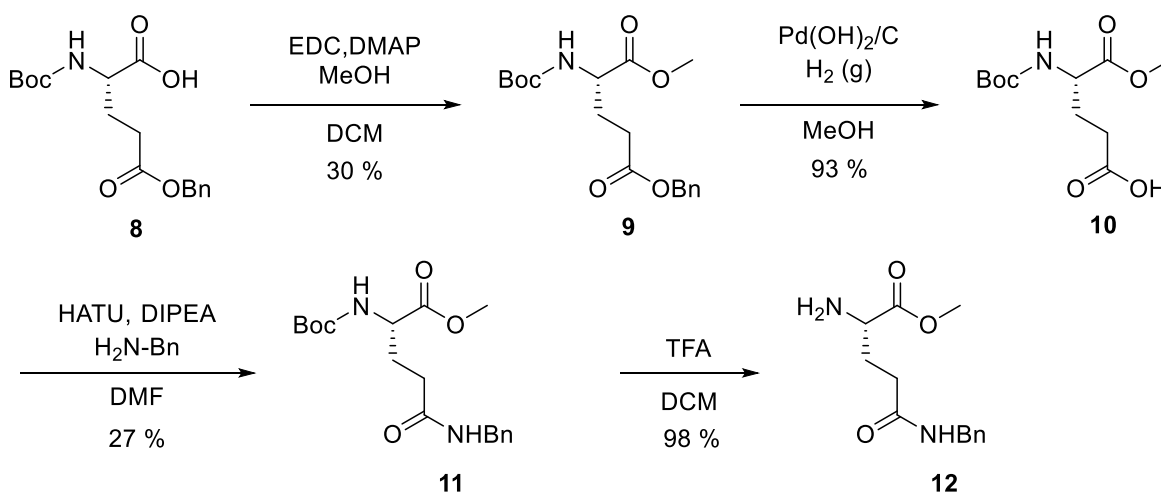
Firstly, the carboxylic acid **7** was prepared. Ethyl isocyanoacetate (**1**), *N*-Cbz-glycine (**2**) and *N*-Boc-L-prolinal (**3**) reacted in a Passerini reaction-amine deprotection-acyl migration (PADAM) sequence, inspired by a published procedure⁶⁰. The obtained β -aminoacyl- α -hydroxyamide **4** was deprotected by catalytic hydrogenation to yield amine **5**, which was then coupled with quinoline-4-carboxylic acid, using the TSTU peptide coupling reagent. This yielded the ester **6**, which was then hydrolyzed, yielding carboxylic acid **7** (Scheme 14).



Scheme 14 – Preparation of carboxylic acid **7**.

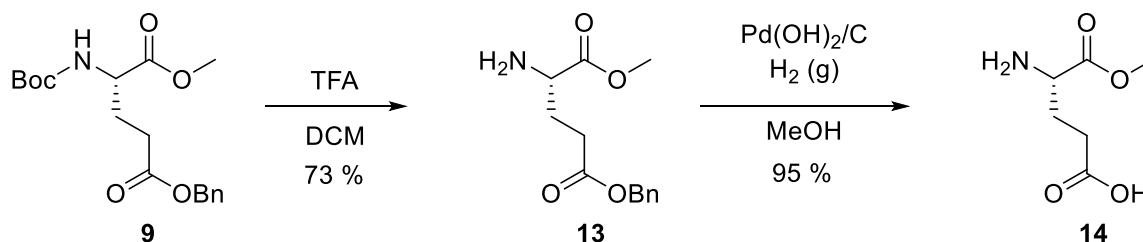
Afterwards, different derivatives of glutamic acid were prepared to achieve intended variations in P2' positions of the final inhibitors. The α -carboxyl of *N*-Boc-L-glutamic acid γ -benzyl ester (**8**) was esterified *via* carbodiimide activation, providing the methyl ester **9**.

The γ -benzyl ester moiety was then catalytically hydrogenolyzed, yielding the carboxylic acid **10**. Subsequent peptide coupling of acid **10** and benzylamine, using HATU, resulted in the formation of benzyl amide **11**, which was finally deprotected by TFA, yielding *N*⁵-benzyl-L-glutamine methyl ester (**12**, Scheme 15).



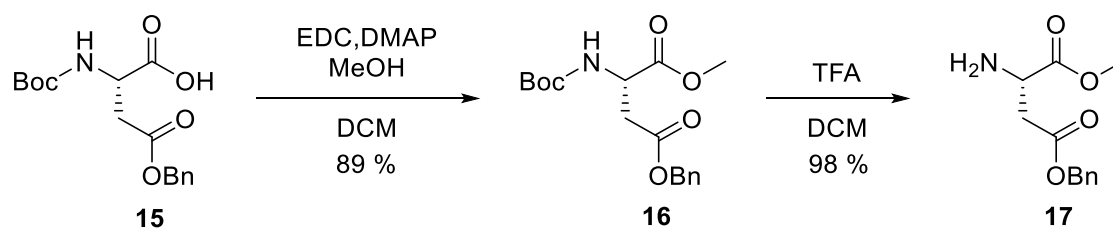
Scheme 15 – Synthesis of *N*⁵-benzyl-L-glutamine methyl ester **12**.

Compound **9** was also used as a precursor for the glutamic acid derivatives **13** and **14**. Firstly, an amine deprotection was carried out, yielding amine **13**, which was then catalytically hydrogenated to obtain compound **14** (Scheme 16).



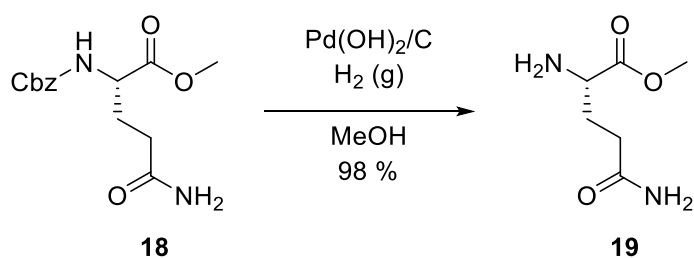
Scheme 16 – Preparation of glutamic acid derivatives **13** and **14**.

The aspartic acid derivative **17** was prepared from *N*-Boc-L-aspartic acid β -benzyl ester (**15**) *via* EDC-mediated esterification, yielding compound **16**, followed by an amine deprotection, forming the final product **17** (Scheme 17).



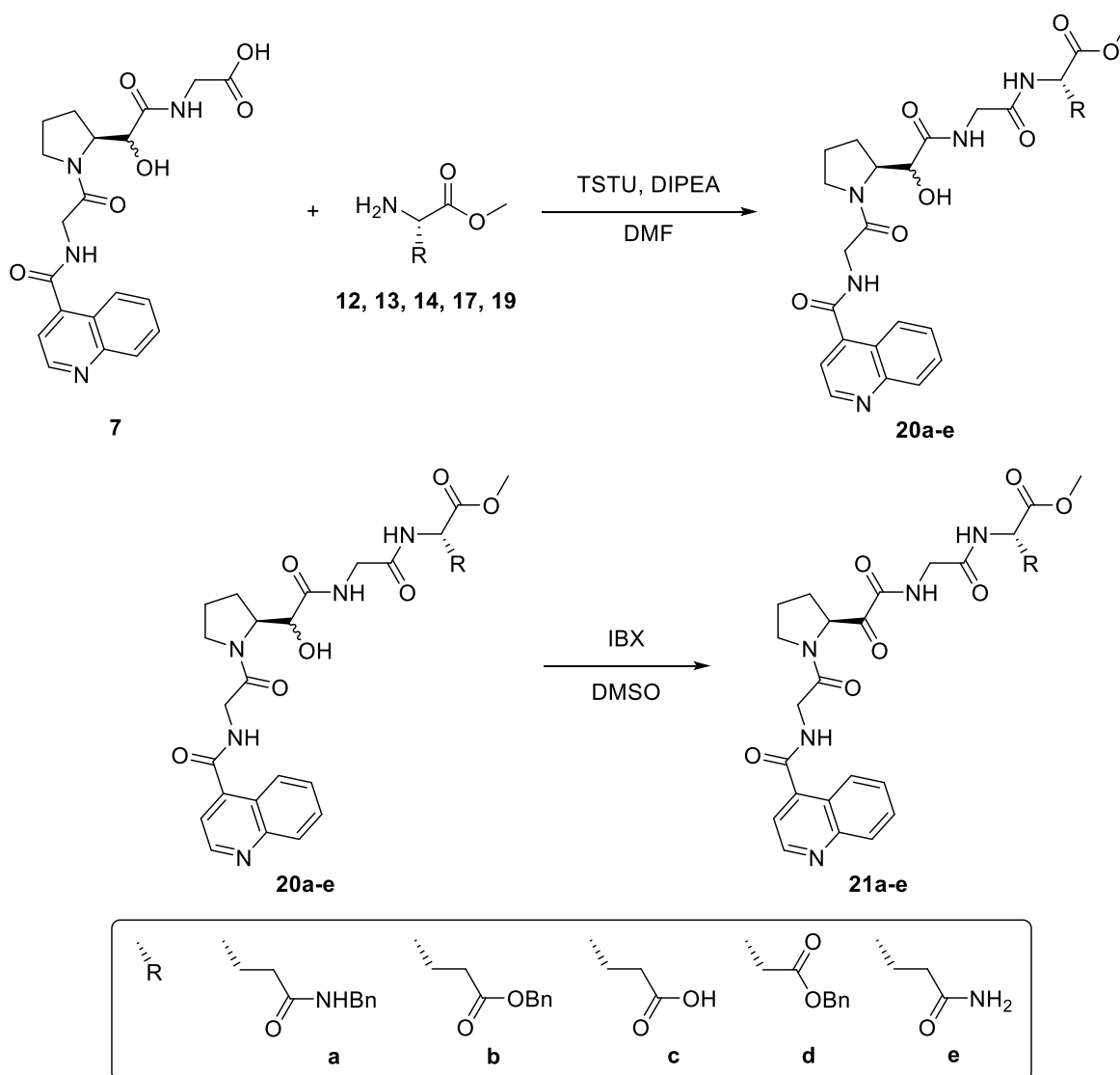
Scheme 17 – Preparation of the aspartic acid derivative **17**.

Methyl L-glutamate (19) was prepared in one step via catalytic hydrogenation of its *N*-protected derivative 18 (Scheme 18).



Scheme 18 – Preparation of the glutamine derivative **19**.

Coupling of compounds **12**, **13**, **14**, **17** and **19** with carboxylic acid **7** provided the α -hydroxyamides **20a-e**, which were then oxidized to final products **21a-e** (Scheme 19, Table 1).

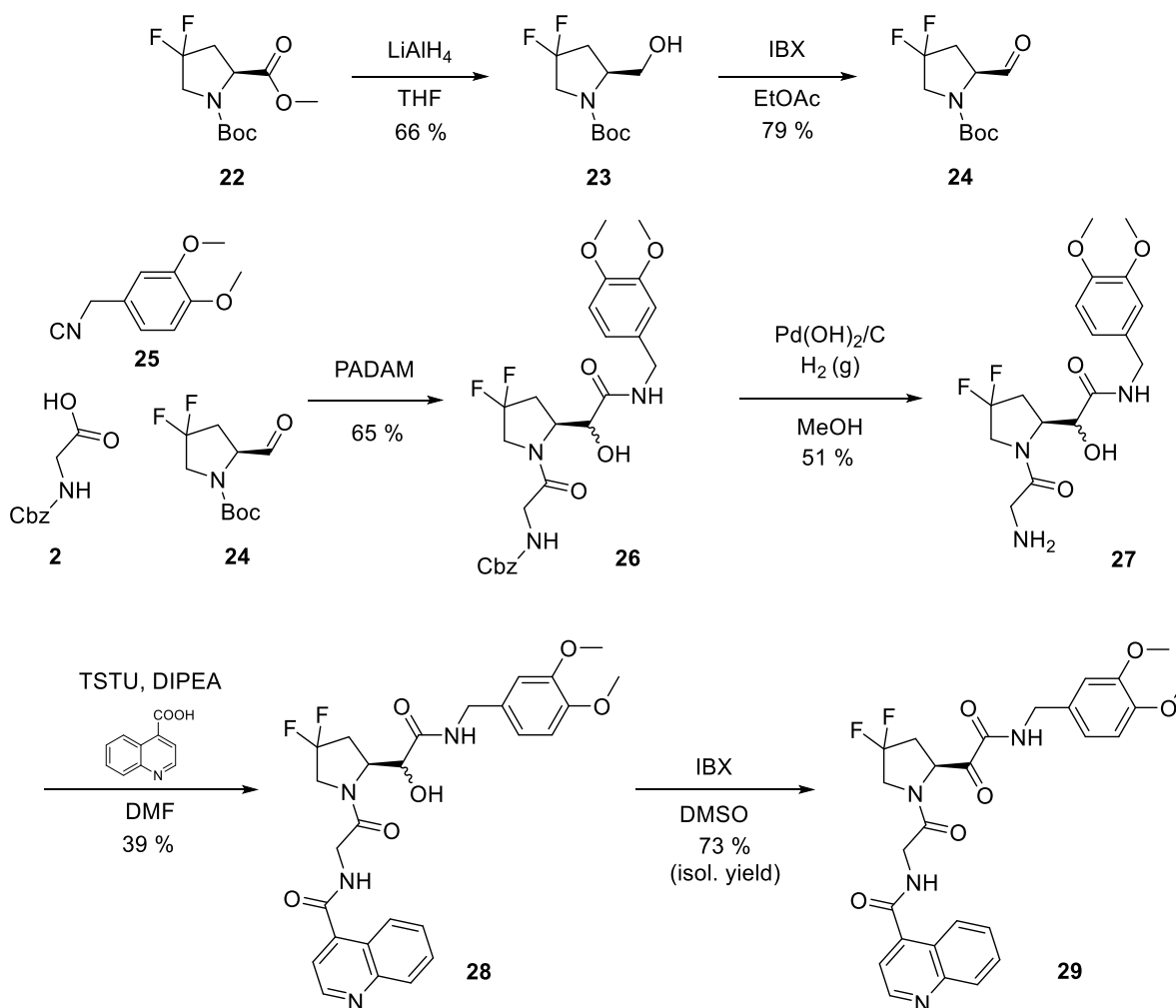


Scheme 19 – Preparation of final compounds **21a-e** from the building blocks **7**, **12**, **13**, **14**, **17** and **19**.

Table 1 – Yields for the preparation of α -hydroxyamides **20a-e** and their oxidation to final inhibitors **21a-e**.

Amine	Peptide coupling product	Peptide coupling yield (%)	Oxidation product	Oxidation isol. yield (%)
12	20a	47	21a	25
13	20b	76	21b	50
14	20c	53	21c	63
17	20d	41	21d	54
19	20e	54	21e	20

Inhibitor **29**, bearing fluorine atoms in the C3-position of the pyrrolidine ring, was prepared from the commercially available methyl ester **22**, which was reduced to the corresponding alcohol **23** and then oxidized to aldehyde **24**. A PADAM sequence (in this case, 3,4-dimethoxybenzyl isocyanide (**25**) was used) was employed, followed by amine deprotection, which yielded compound **27**. A TSTU coupling with quinoline-4-carboxylic acid, followed by an IBX oxidation yielded the final inhibitor **29** (Scheme 20). The synthesis of aldehyde **24** was optimized for a reaction scale-up in the future (see page 38).



Scheme 20 – Synthesis of the fluorine-substituted inhibitor **29**.

Reference inhibitors **R1** and **R2** (page 29) were prepared according to published procedures^{3,80}. Reference inhibitor **R3**, the previously mentioned lead inhibitor established in the Konvalinka lab, was prepared from *N*-Boc-L-prolinal by identical procedure as is depicted in Scheme 20. All reference compounds **R1-R3** were then characterized by ¹H and ¹³C NMR spectroscopy, UPLC/MS and were used for comparison with final inhibitors **21a-e** and **29**.

3.2 Evaluation of the Synthesis

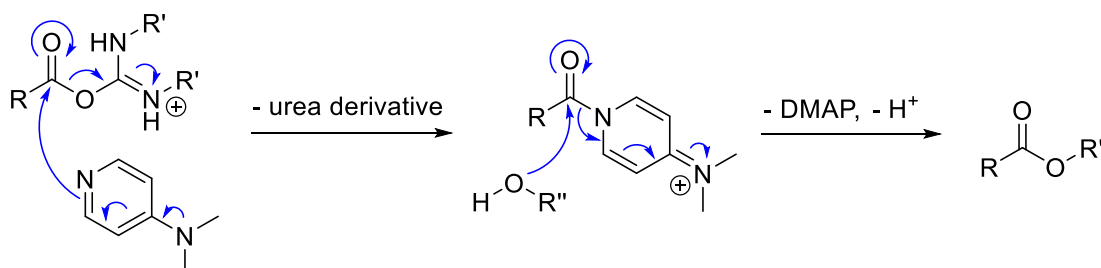
The α -ketoamide inhibitors **20a-e** and **29**, two reference inhibitors with a nitrile warhead (**R1** and **R2**) and one reference α -ketoamide inhibitor **R3** were prepared.

The synthesis of carboxylic acid **7** was already optimized within previous work on this project, so no optimization of reaction conditions was needed. The synthesis of amine building blocks **12**, **13**, **14**, **17** and **19**, had to be designed from start to finish. The synthetic plan was built from the starting materials readily available in our laboratory.

All the proposed transformations and reaction conditions were based either on standard synthetic procedures (e.g., *N*-Boc deprotection, benzyl ester hydrogenolysis), previous laboratory experience (e.g., peptide coupling reactions, IBX oxidation) or related literature. However, some synthetic transformations had to be optimized.

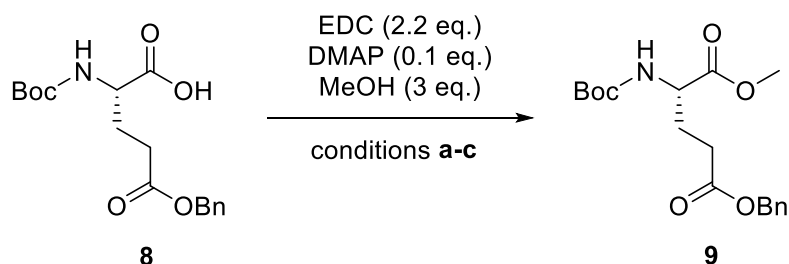
3.2.1 EDC Esterification Optimization

For the esterification of *N*-Boc-L-glutamic acid γ -benzyl ester (**8**) (Scheme 15), a suitable method had to be found. As was discussed in paragraph 1.2.5.1 (page 21), carbodiimides can be used for the activation of carboxylic acids. Commonly, they are used for the synthesis of amides. However, they can also be employed for esterifications of carboxylic acids. The main issue with esterification reactions is the difference in nucleophilicity between amines and alcohols. The activated *O*-acylisourea reacts readily with amines to form amides, but its reaction with alcohols is significantly slower, which gives rise to other side reactions, namely to the rearrangement to an unreactive *N*-acylurea. For this reason, 4-dimethylaminopyridine (DMAP) is usually added as a catalyst. DMAP is a stronger nucleophile than alcohols and reacts with the active *O*-acylisourea, forming an activated amide which is not capable of the rearrangement to *N*-acylurea. This activated amide then reacts with the alcohol, generating the desired ester⁸¹ (Scheme 21).



Scheme 21 – Mechanism of the DMAP-mediated esterification of carboxylic acids.

During the esterification of *N*-Boc L-glutamic acid γ -benzyl ester (**8**), a small-scale screening of solvents was performed (Scheme 22). In all reactions (**a-c**), 2.2 equivalents of EDC hydrochloride were used for the activation of carboxylic acid **8** in the presence of 0.1 equivalents of DMAP followed by an esterification with excess (3 eq.) MeOH. The chosen solvents were dichloromethane (**a**), methanol (**b**) and *N,N*-dimethylformamide (**c**).



Scheme 22 – Optimization of the EDC esterification of acid **8**.

The reaction mixtures were analyzed by UPLC/MS. The analyses have shown the presence of the desired methyl ester peak and an unknown side-product peak. Both peaks were then integrated, and a total area percentage was calculated (Table 2).

Table 2 – Conversion of the starting material **8** to the methyl ester **9**. The total area percentages were determined from the UPLC chromatograms using absorbance at 210 nm.

Entry	Solvent	Reaction conditions	Product 9 (%)	Side-product (%)
a	DCM	RT, 6 h	87	13
b	MeOH	RT, 6 h	82	18
c	DMF	RT, 6 h	50	50

Subsequent literature analysis has shown that the DMAP-mediated acyl transfer (Scheme 21) occurs much slower in aprotic polar solvents⁸², promoting the rearrangement reaction of the reactive *O*-acylisourea to the unreactive *N*-acylurea. The side-product peak MS spectrum corresponded with the *N*-acylurea monoisotopic mass. Since a drastic increase in the formation of the observed side-product in reaction (**c**) was also observed, the side-product was most likely the unreactive *N*-acylurea. As a result of this screening, dichloromethane was chosen as the solvent of choice for EDC esterifications.

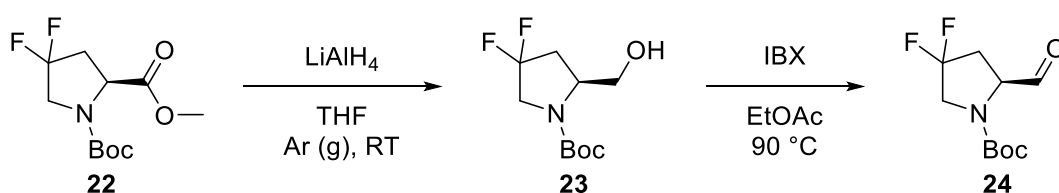
3.2.2 *N*-Boc-4,4-difluoro-L-prolinal Synthesis Optimization

Due to commercial unavailability of the 4,4-difluoroaldehyde **24**, an alternative synthetic approach based on the available methyl ester **22** had to be employed. Even though most published transformations are based on a full reduction to the alcohol and a subsequent oxidation to the aldehyde, a partial reduction with DIBAL-H was tried out, as a one-step preparation of the aldehyde would be convenient. However, the transformation was unsuccessful, most likely due to difficult control of reaction temperature – too low temperatures reduce reactivity, too high temperatures result in the full reduction to an alcohol⁸³.

Therefore, the second approach was chosen and a reduction with LiAlH₄ in tetrahydrofuran with an aqueous quench was performed. Upon TLC and UPLC/MS analyses it was apparent, that a significant amount of the product had its *N*-Boc protecting group hydrolyzed under the strongly basic conditions.

To mitigate the Boc cleavage, strictly anhydrous conditions were used (anhydrous solvent, inert atmosphere). The reaction was quenched with ethyl acetate instead of water to avoid basic hydrolysis of the protecting group. For the same reason, neutralization with a HCl solution in ethyl acetate was used to protonate the lithium alkoxide, yielding the alcohol **23**.

Next, the oxidation reaction conditions were optimized. An oxidation with Dess-Martin periodinane (DMP) was tried out but has resulted in incomplete conversion and a formation of multiple products (TLC analysis). Subsequent NMR spectroscopy measurements have shown partial degradation of the reagent. Therefore, an IBX oxidation in dimethyl sulfoxide was performed and showed complete conversion after heating to 90 °C. The oxidation was also performed in a suspension of IBX in ethyl acetate at reflux temperatures (inspired by literature⁸⁴), which also led to complete conversion. These reaction conditions were then chosen, due to an easier workup by only filtration and evaporation, as IBX is insoluble in virtually all organic solvents except dimethyl sulfoxide (**Scheme 23**).



Scheme 23 – Optimized synthesis of the difluorinated aldehyde **24**.

3.3 Inhibitory Potencies of Target Compounds

Table 3 lists the IC₅₀ values for reference inhibitors **R1-R3**, which were determined against FAP, DPPIV and PREP by Mgr. Tereza Ormsby, Ph. D in the Konvalinka lab.

Table 4 displays the obtained IC₅₀ values of inhibitors **21a-e** and **29**.

The design of compounds **21a-e** was based on various modifications in the P2' position, where various derivatives of glutamic acid, aspartic acid and glutamine were incorporated. The remainder of their structure comes from the state-of-the-art FAP inhibitors **R1**, **R2**.

It is apparent that inhibitors **21a** and **21b**, bearing the benzyl amide and benzyl ester moieties, respectively, have the highest inhibitory potencies with both of their IC₅₀ values being below 3 nM. This indicates that the presence of an aromatic moiety in the P2' position side-chain is likely desired. Shortening the side-chain length by one carbon (compound **21d**), however, led to a 31-fold decrease in potency. This might show that a minimal side-chain length is necessary, probably to ensure enough flexibility between the oligopeptide backbone and its side-chain moieties.

Removal of the aromatic side-chain moiety (compounds **21c** and **21e**, respectively) led to an inhibitory potency decrease by one order of magnitude, on average.

Out of the five α -ketoamide inhibitors **21a-e**, compounds **21a** and **21b** show the greatest inhibitory potency. It must be noted, that even though compound **21b** has a sub-nanomolar IC₅₀ of 0.590 nM, it bears a benzyl ester group, which could be subject to hydrolysis *in vivo*. Subsequent stability measurements have shown that compound **21b** is stable in human plasma but undergoes rapid degradation in mouse plasma. For this reason, the more potent and more stable inhibitor **R3** was chosen for further studies.

Comparison with the reference inhibitors **R1** and **R2** shows that both inhibitors **21a** and **21b** have a higher inhibitory potency towards FAP. However, the selectivities towards FAP over its homologs DPPIV and PREP have yet to be investigated.

The trend of increasing affinity towards FAP by the introduction of fluorine atoms to the pyrrolidine C3-position was not observed in the case of inhibitor **29**, where it led to only a 1.3-fold increase in potency. This substitution also has not led to a significant improvement in FAP/PREP selectivity of inhibitor **29** (SI (FAP/PREP) = 2.4), compared to reference inhibitor **R3** (SI (FAP/PREP) = 2.1).

Table 3 - Half-maximal inhibitory concentrations towards FAP, DPPIV and PREP for reference inhibitors **R1-R3**.

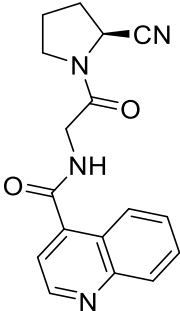
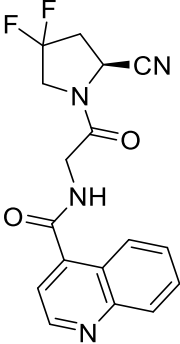
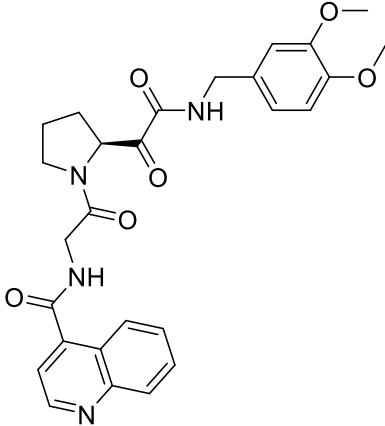
No.	Structure	IC ₅₀ [nM]		
		FAP	DPPIV	PREP
R1		28.5	> 4000	660
R2		4.27	> 4000	670
R3		0.191	> 4000	0.4

Table 4 - Half-maximal inhibitory concentrations towards FAP for inhibitors **21a-e** and towards FAP and PREP for inhibitor **29**.

No.	R	X	IC ₅₀ [nM]
21a		H	2.15
21b		H	0.590
21c		H	16.1
21d		H	18.6
21e		H	18.4
29		F	0.146 (FAP) 0.349 (PREP)

4 Summary and Conclusion

Within this thesis, a total of six novel α -ketoamide FAP inhibitors **21a-e** and **29** were designed. These compounds are part of a broader FAP inhibitor SAR study, which investigates the effect of various structural modifications in the P1' and P2' positions on the inhibitory potencies towards FAP and on the selectivity towards FAP over its homologs DPPIV and PREP.

Five FAP inhibitors **21a-e**, bearing different derivatives of glutamic acid, aspartic acid, and glutamine, were successfully synthesized *via* a proposed synthetic plan, which comprised of known and well-established reactions, but also some synthetic transformations, whose reaction conditions had to be optimized. All inhibitors were fully characterized by ^1H and ^{13}C NMR spectroscopy, UPLC/MS, HRMS, IR spectroscopy, elemental analysis (some exceptions due to insufficient material), and optical rotation measurement. Most synthetic intermediates were characterized by ^1H and ^{13}C NMR spectroscopy and UPLC/MS.

The inhibitory potencies of prepared inhibitors were determined using a fluorogenic substrate assay. The results indicate the discovery of two low-nanomolar FAP inhibitors **21a** (2.15 nM) and **21b** (0.590 nM), both of which show greater inhibitory potencies than reference inhibitors **R1** and **R2**. Both compounds **21a** and **21b** have an aromatic moiety in position P2', which gives rise to a hypothesis, that the presence of an aromatic or other non-polar moiety in position P2' is beneficial for inhibitory potency. The removal of aromatic groups led to a decrease in inhibitory potencies, further supporting this hypothesis.

Inhibitor **29**, a derivative of the lead α -ketoamide inhibitor **R3** with fluorine atoms in the pyrrolidine C3-position was also prepared and characterized to investigate the potential changes of inhibitory potency and selectivity associated with the introduction of fluorine atoms to the pyrrolidine ring. The results indicate only a slight increase in inhibitory potency and no improvement in FAP/PREP selectivity, compared to reference inhibitor **R3**.

5 Experimental Section

5.1 Chemicals, Materials and Equipment

Used solvents were manufactured by Sigma-Aldrich (*N,N*-dimethylformamide; dimethyl sulfoxide), TCI Chemicals (dichloromethane), VWR Chemicals (methanol), PENTA Chemicals (cyclohexane; ethyl acetate) and Fischer Chemical (acetonitrile). Deuterated solvents for NMR experiments were supplied by Eurisotop and Sigma-Aldrich.

Starting materials and reagents were supplied by Fluorochem (*N*-Boc-L-prolinal; *N*-benzyloxycarbonylglycine; quinoline-4-carboxylic acid; *N*-Boc-4,4-difluoro-L-proline methyl ester; TFA; HATU; TSTU; EDC), Sigma-Aldrich (ethyl isocyanoacetate; TEA; DIPEA; DMP; Pd(OH)₂/C) and Merck (DMAP). Lab-made IBX was used.

For TLC analyses, aluminium TLC silica 60 F₂₅₄ plates from Merck were used. Normal phase liquid chromatography was done with a 40-63 μm silica gel from VWR Chemical. Reversed phase flash liquid chromatographies were carried out with RediSep Rf C18 Gold columns of various sizes on a Teledyne ISCO CombiFlash Rf-200 chromatograph. Preparative HPLC was carried out on an ECOM ECS28P0X Compact Preparative System with a Bischoff ProntoSIL ace-EPS column (10 μm, 250 x 20.0 mm) and a Bischoff ProntoSIL ace-EPS guard column (10 μm, 50 x 20.0 mm). All mobile phase compositions and gradients are specified for each compound in the next section.

UPLC/MS analyses were performed on a Waters UPLC H-Class Core System (Waters Acquity UPLC BEH C18 column (1.7 μm, 2.1 x 100 mm), Waters Acquity UPLC PDA diode array 190-800 nm detector, Waters SQD2 Mass spectrometer, MassLynx Mass Spectrometry Software).

¹H and ¹³C NMR spectra of intermediate compounds were recorded on a Bruker Avance III HD 400 MHz spectrometer, except for α-hydroxyamides **20a-e** which were characterized only by UPLC/MS. ¹H and ¹³C NMR spectra of final compounds **21a-e** were recorded on a Bruker Avance III 500 MHz spectrometer. NMR signal assignment was performed using a combination of 1D-NMR (¹H, APT) and 2D-NMR (COSY, HSQC, HMBC, NOESY) experiments. Chemical shifts are given in ppm. Figure 17 shows the numbering of atoms for the assignment of NMR signals of final compounds **21a-e** and **29**.

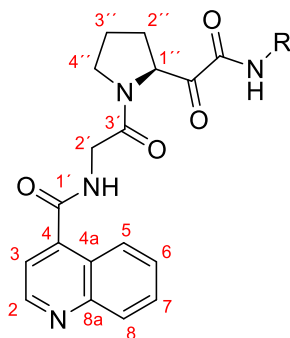


Figure 17 – Numbering of atoms for the assignment of NMR signals for compounds **21a-e**.

High resolution MS analyses were performed on a LQT Orbitrap XL Mass spectrometer (Thermo Fisher Scientific) equipped with an electrospray ion source. Optical rotations were measured on an Autopol IV polarimeter (Rudolph Research Analytical). Infrared spectra were measured by thin film IR spectroscopy on a Nicolet 6700 FT-IR spectrometer (Thermo Fisher Scientific). CHN elemental analyses were performed on an PE 2400 Series II Elemental Analyzer (Perkin Elmer), fluorine elemental analyses were performed *via* ion-selective electrode measurements.

5.2 Synthesis and Characterization of Compounds

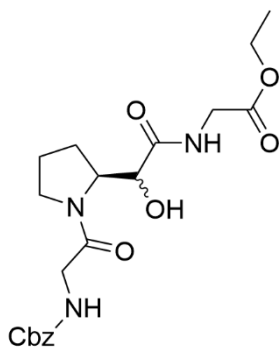
General procedure 1 – TSTU coupling

1.0 eq of carboxylic acid and 1.0 eq of TSTU were dissolved in anhydrous *N,N*-dimethylformamide. 5.0 eq of anhydrous DIPEA were added and the mixture was stirred at RT for 1 hour. Afterwards, 1.0 eq of amine was added and the mixture was stirred at RT overnight for 16 hours. The product was isolated by reversed phase flash chromatography with a gradient from 0.1% TFA to acetonitrile (gradient specified per each compound). Corresponding fractions were then lyophilized.

General procedure 2 – IBX oxidation

1.0 eq of α -hydroxyamide and 3.0 eq of IBX were dissolved in anhydrous dimethyl sulfoxide. The mixture was stirred at RT for 16 hours, after which the product was isolated by preparative reversed phase HPLC with a gradient from 0.1% TFA to acetonitrile. Corresponding fractions were then lyophilized.

Ethyl (S)-(2-(1-(((benzyloxy)carbonyl)glycyl)pyrrolidin-2-yl)-2-hydroxyacetyl)glycinate (4)



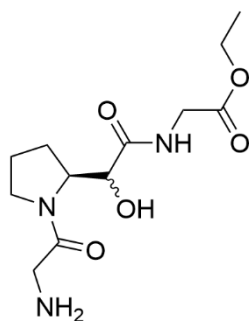
517 mg of ethyl isocyanoacetate (4.58 mmol, 1.0 eq), 1.05 g of *N*-benzyloxycarbonylglycine (5.02 mmol, 1.1 eq) and 1.00 g of *N*-Boc-L-prolinal (5.02 mmol, 1.1 eq) were dissolved in 10 mL of anhydrous dichloromethane. The mixture was stirred at RT for 20 hours and 2 mL of TFA were added afterwards. After 30 minutes, complete deprotection of the Passerini reaction product was observed (UPLC/MS). The reaction mixture was evaporated and dried *in vacuo* for 1 hour. The mixture was then redissolved in 5 mL of anhydrous dichloromethane, cooled to 0 °C and a mixture of 5 mL TEA and 15 mL anhydrous dichloromethane was added dropwise. The reaction mixture was then warmed up to RT and stirred for 1 hour, until complete *O*-*N* transacylation was observed (UPLC/MS). The mixture was diluted with dichloromethane to a total volume of 50 mL and washed with distilled water (4 x 50 mL) and brine (50 mL). The organic layer was dried over anhydrous MgSO₄, filtered, evaporated and dried *in vacuo*, which yielded 1.33 g (69 %) of compound **4** as a brown oil.

UPLC/MS – R_{t1} = 3.670 min, R_{t2} = 3.722 min, ESI+ [M+H]⁺ = 422.368

¹H NMR (400 MHz, CDCl₃) δ 7.46 (dt, *J* = 25.3, 5.9 Hz, 1H), 7.28 – 7.20 (m, 5H), 6.04 – 5.87 (m, 1H), 5.54 (s, 1H), 5.01 (d, *J* = 2.2 Hz, 2H), 4.20 (d, *J* = 2.3 Hz, 1H), 4.07 (dq, *J* = 17.8, 7.1 Hz, 2H), 3.97 – 3.79 (m, 4H), 3.47 – 3.21 (m, 2H), 2.18 (ddt, *J* = 14.0, 10.1, 5.4 Hz, 1H), 2.03 – 1.24 (m, 4H), 1.17 (t, *J* = 7.2 Hz, 3H).

¹³C NMR (100 MHz, CDCl₃) δ 172.46, 169.97, 169.67, 156.52, 136.38, 128.46, 128.08, 127.99, 73.20, 66.88, 62.07, 61.38, 46.83, 43.62, 40.87, 26.40, 23.98, 14.12

Ethyl (S)-(2-(1-glycylpyrrolidin-2-yl)-2-hydroxyacetyl)glycinate (5)



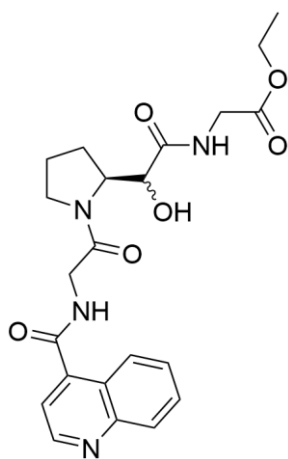
307 mg of compound **4** (0.78 mmol, 1.0 eq) were dissolved in 5 mL of methanol and a catalytical amount of Pd(OH)₂/C was added. The reaction mixture was stirred at RT for 3 hours under hydrogen atmosphere, after which complete hydrogenolysis of compound **4** was observed. The reaction mixture was filtered through a syringe filter, evaporated, and dried *in vacuo*, which yielded 207 mg (99 %) of compound **5** as a brown amorphous solid.

UPLC/MS – $R_{t1} = 2.387$ min, $R_{t2} = 2.512$ min, ESI+ $[M+H]^+ = 288.196$

1H NMR (400 MHz, $CDCl_3$) δ 8.03 (s, 1H), 7.62 (dt, $J = 27.8, 5.9$ Hz, 2H), 4.81 (s, 1H), 4.61 (d, $J = 2.1$ Hz, 1H), 4.21 (d, $J = 3.9$ Hz, 1H), 4.16 – 4.06 (m, 2H), 3.93 (t, $J = 4.9$ Hz, 2H), 3.58 (d, $J = 4.5$ Hz, 2H), 3.34 (d, $J = 9.0$ Hz, 2H), 2.12 – 1.66 (m, 4H), 1.20 (t, $J = 7.2$ Hz, 3H).

^{13}C NMR (100 MHz, $CDCl_3$) δ 172.73, 171.33, 169.65, 72.78, 71.42, 61.32, 46.56, 43.01, 40.80, 26.26, 23.81, 14.03.

Ethyl (*S*)-(2-hydroxy-2-(1-((quinoline-4-carbonyl)glycyl)pyrrolidin-2-yl)acetyl)glycinate (6)



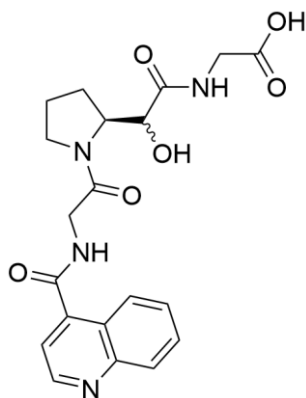
61 mg (54 %) of compound **6** as a white amorphous solid were prepared from 73 mg (0.25 mmol, 1.0 eq) of amine **5** by General procedure 1 (chromatography gradient 0 → 40 % acetonitrile).

UPLC/MS – $R_{t1} = 3.025$ min, $R_{t2} = 3.085$ min, ESI+ $[M+H]^+ = 443.286$

1H NMR (400 MHz, $CDCl_3$) δ 9.68 (s, 1H), 9.09 (t, $J = 5.1$ Hz, 1H), 8.41 (t, $J = 5.1$ Hz, 1H), 8.32 (dd, $J = 8.6, 1.5$ Hz, 1H), 8.28 (t, $J = 7.1$ Hz, 1H), 8.19 (d, $J = 9.0$ Hz, 1H), 7.91 (t, $J = 5.6$ Hz, 1H), 7.84 (dddd, $J = 8.5, 7.0, 2.6, 1.3$ Hz, 1H), 7.72 – 7.64 (m, 1H), 4.35 – 4.25 (m, 1H), 4.20 (d, $J = 17.2$ Hz, 2H), 4.06 (q, $J = 7.2$ Hz, 2H), 4.02 (d, $J = 7.2$ Hz, 1H), 3.90 (t, $J = 5.2$ Hz, 2H), 3.57 – 3.40 (m, 2H), 2.17 – 1.92 (m, 2H), 1.92 – 1.77 (m, 2H), 1.16 (t, $J = 7.0$ Hz, 3H).

^{13}C NMR (100 MHz, $CDCl_3$) δ 172.84, 169.68, 168.71, 165.45, 148.79, 145.40, 140.11, 134.00, 130.19, 126.60, 125.62, 122.63, 119.86, 72.23, 61.84, 61.48, 47.08, 42.75, 40.93, 26.23, 23.98, 14.05.

(S)-2-hydroxy-2-(1-((quinoline-4-carbonyl)glycyl)pyrrolidin-2-yl)acetyl)glycine (7)



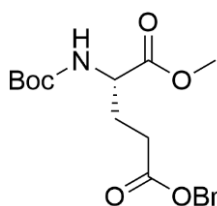
1.30 g of ethyl ester **6** (2.94 mmol, 1.0 eq) were dissolved in 10 mL of ethanol and 1 mL of 10% aqueous KOH was added. The reaction mixture was stirred at RT for 2 hours, after which complete ester hydrolysis was observed (UPLC/MS). The mixture was neutralized by dropwise addition of 10% aqueous HCl, evaporated, redissolved in acetonitrile and purified by flash chromatography on a reversed phase C18 column (gradient from 0.1% TFA (aq.) to acetonitrile, 0 → 50 %) The corresponding fractions were lyophilized and 542 mg (44 %) of compound **7** was obtained as a brown amorphous solid.

UPLC/MS – $R_{t1} = 2.647$ min, $R_{t2} = 2.710$ min, ESI+ $[M+H]^+ = 415.312$

¹H NMR (400 MHz, MeOD) δ 9.15 (dd, $J = 5.0, 1.2$ Hz, 1H), 8.58 (d, $J = 8.5$ Hz, 1H), 8.22 (d, $J = 8.5$ Hz, 1H), 8.05 (ddt, $J = 8.7, 7.0, 1.7$ Hz, 1H), 7.98 – 7.93 (m, 1H), 7.89 (ddd, $J = 8.3, 7.0, 1.2$ Hz, 1H), 4.51 (d, $J = 4.6$ Hz, 1H), 4.44 (q, $J = 4.0, 3.3$ Hz, 1H), 4.41 – 4.23 (m, 2H), 4.06 – 3.93 (m, 2H), 3.69 – 3.58 (m, 2H), 2.37 – 2.13 (m, 2H), 2.13 – 1.87 (m, 2H).

¹³C NMR (100 MHz, MeOD) δ 174.15, 171.40, 168.01, 167.32, 147.38, 147.20, 143.21, 132.67, 129.05, 126.40, 125.29, 124.46, 119.39, 70.84, 60.86, 46.73, 42.15, 40.18, 25.88, 23.69.

5-benzyl 1-methyl (tert-butoxycarbonyl)-L-glutamate (9)



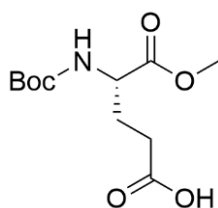
2.00 g of *N*-Boc-L-glutamic acid γ -benzyl ester (5.93 mmol, 1.0 eq), 1.37 g of EDC hydrochloride (7.12 mmol, 1.2 eq) and 73 mg of DMAP (0.59 mmol, 0.1 eq) were dissolved in 10 mL of anhydrous dichloromethane. Afterwards, 0.72 mL of anhydrous methanol (17.8 mmol, 3.0 eq) was added and the reaction mixture was stirred overnight for 16 hours. The mixture was diluted with 50 mL of ethyl acetate, washed with 10% aqueous KHSO_4 (3 x 50 mL) and brine (1 x 50 mL), dried over anhydrous MgSO_4 , filtered and evaporated. The crude mixture was redissolved in cyclohexane and purified by flash chromatography on a silica column (gradient from cyclohexane to ethyl acetate, 0 → 50 %). Corresponding fractions were pooled and evaporated. A fraction collector malfunction occurred, which resulted in only a partial recovery of 677 mg (30 %) of compound **9** as a colorless oil.

UPLC/MS – $R_t = 4.652$ min, ESI+ [M-Boc+H]⁺ = 252.209

¹H NMR (400 MHz, CDCl₃) δ 7.32 – 7.22 (m, 5H), 5.05 (s, 2H), 4.28 (q, $J = 7.5$ Hz, 1H), 3.66 (s, 3H), 2.47 – 2.29 (m, 2H), 2.14 (tt, $J = 13.8, 6.3$ Hz, 1H), 1.89 (dtd, $J = 14.5, 8.3, 6.4$ Hz, 1H), 1.36 (s, 9H).

¹³C NMR (100 MHz, CDCl₃) δ 172.68, 172.51, 155.35, 135.75, 128.58, 128.30, 128.27, 80.04, 66.54, 52.81, 52.43, 30.32, 28.29, 27.79.

(S)-4-((tert-butoxycarbonyl)amino)-5-methoxy-5-oxopentanoic acid (10)



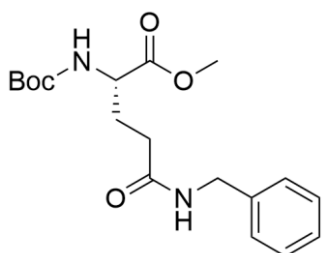
202 mg of compound **9** (0.58 mmol, 1.0 eq) were dissolved in 5 mL of methanol and a catalytical amount of Pd(OH)₂/C was added. The reaction mixture was stirred at RT for 3 hours under hydrogen gas, after which complete hydrogenolysis of compound **9** was observed (UPLC/MS). The reaction mixture was filtered through a syringe filter, evaporated and dried *in vacuo*, which yielded 140 mg (93 %) of compound **10** as a colorless oil.

UPLC/MS – $R_t = 3.451$ min, ESI+ [M-Boc+H]⁺ = 162.085

¹H NMR (400 MHz, CDCl₃) δ 8.84 (s, 1H), 5.10 (d, $J = 8.4$ Hz, 1H), 4.30 (d, $J = 6.6$ Hz, 1H), 3.69 (s, 3H), 2.52 – 2.29 (m, 2H), 2.13 (dq, $J = 13.5, 7.0$ Hz, 1H), 1.96 – 1.82 (m, 1H), 1.37 (s, 9H).

¹³C NMR (100 MHz, CDCl₃) δ 177.61, 172.63, 155.51, 80.29, 52.70, 52.50, 29.97, 28.27, 27.74.

Methyl N⁵-benzyl-N²-((tert-butoxycarbonyl)-L-glutamate (11)



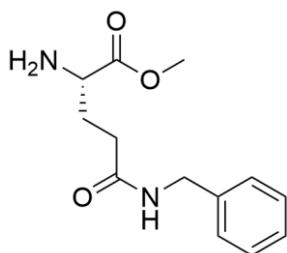
155 mg of carboxylic acid **10** (0.59 mmol, 1.0 eq) and 197 mg of HATU (0.59 mmol, 1.0 eq) were dissolved in 3 mL of anhydrous *N,N*-dimethylformamide. 0.27 mL of anhydrous DIPEA (1.77 mmol, 3.0 eq) were added and the mixture was stirred at RT for 10 minutes, after which 57 μL of benzylamine (0.59 mmol, 1.0 eq) were added. The mixture was then stirred at RT overnight for 16 hours and purified by flash chromatography on a reversed phase C18 column (gradient from 0.1% TFA (aq.) to acetonitrile, 0 → 70 %). A fraction collector malfunction occurred, which resulted in only a partial recovery of 49 mg (27 %) of compound **11** as a white amorphous solid.

UPLC/MS – $R_t = 4.088$ min, ESI+ [M-Boc+H]⁺ = 251.233, [M+Na]⁺ = 373.334

¹H NMR (400 MHz, CDCl₃) δ 7.33 – 7.13 (m, 5H), 6.62 (s, 1H), 5.39 – 5.23 (m, 1H), 4.37 (d, *J* = 5.6 Hz, 2H), 4.21 (q, *J* = 7.2, 6.6 Hz, 1H), 3.66 (s, 3H), 2.26 (t, *J* = 7.1 Hz, 2H), 2.13 (dtd, *J* = 14.6, 7.4, 4.5 Hz, 1H), 1.95 – 1.80 (m, 1H), 1.35 (s, 9H).

¹³C NMR (100 MHz, CDCl₃) δ 172.63, 172.31, 155.92, 137.91, 128.69, 127.82, 127.53, 80.31, 52.92, 52.52, 43.83, 32.46, 29.17, 28.28.

Methyl *N*⁵-benzyl-L-glutamate (**12**)



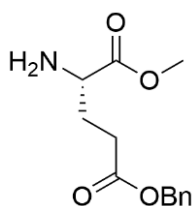
49 mg of compound **11** (0.14 mmol, 1.0 eq) were dissolved in 1 mL of dichloromethane and 1 mL of TFA was added. The mixture was stirred at RT for 1 hour. After complete conversion (UPLC/MS), the mixture was evaporated and dried *in vacuo*, which yielded 50 mg (98 %) of compound **12** TFA salt as a colorless oil.

UPLC/MS – *R*_t = 2.792 min, ESI+ [M+H]⁺ = 251.206

¹H NMR (400 MHz, CDCl₃) δ 8.61 (s, 3H), 7.23 (s, 1H), 7.20 – 7.07 (m, 5H), 4.21 (d, *J* = 5.2 Hz, 2H), 3.97 (d, *J* = 5.9 Hz, 1H), 3.59 (s, 3H), 2.38 (d, *J* = 6.9 Hz, 2H), 2.25 – 2.14 (m, 1H), 2.09 (d, *J* = 5.0 Hz, 1H).

¹³C NMR (100 MHz, CDCl₃) δ 172.61, 169.64, 137.55, 128.62, 127.51, 127.49, 53.30, 52.63, 43.67, 31.54, 25.80.

5-benzyl 1-methyl L-glutamate (**13**)



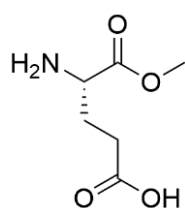
159 mg of compound **9** (0.45 mmol, 1.0 eq) were dissolved in 1 mL of dichloromethane and 1 mL of TFA was added. The mixture was stirred at RT for 1 hour. After complete conversion (UPLC/MS), the mixture was evaporated and dried *in vacuo*, which yielded 120 mg (73 %) of compound **13** TFA salt as a colorless oil.

UPLC/MS – *R*_t = 3.106 min, ESI+ [M+H]⁺ = 252.202;

¹H NMR (400 MHz, CDCl₃) δ 8.30 (bs, 3H), 7.26 (tdt, *J* = 8.1, 5.3, 2.5 Hz, 5H), 5.04 (s, 2H), 4.16 (dd, *J* = 7.1, 5.2 Hz, 1H), 3.70 (s, 3H), 2.59 (t, *J* = 6.4 Hz, 2H), 2.49 – 2.26 (m, 1H), 2.26 – 2.11 (m, 1H).

¹³C NMR (100 MHz, CDCl₃) δ 173.50, 169.30, 135.01, 128.65, 128.59, 128.38, 67.46, 53.60, 52.76, 30.18, 24.96.

(S)-4-amino-5-methoxy-5-oxopentanoic acid (**14**)



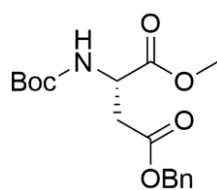
157 mg of compound **13** TFA salt (0.43 mmol, 1.0 eq) were dissolved in 5 mL of methanol and a catalytical amount of Pd(OH)₂/C was added. The reaction mixture was stirred at RT overnight for 16 hours under a hydrogen atmosphere, after which complete hydrogenolysis of compound **13** was observed (UPLC/MS). The reaction mixture was filtered through a syringe filter, evaporated and dried *in vacuo*, which yielded 112 mg (95 %) of compound **14** TFA salt as a light blue oil.

UPLC/MS – R_t = 0.586 min, ESI+ [M+H]⁺ = 162.080

¹H NMR (400 MHz, D₂O) δ 4.20 (dd, *J* = 7.4, 6.3 Hz, 1H), 3.84 (s, 3H), 2.64 (td, *J* = 7.1, 1.1 Hz, 2H), 2.35 – 2.14 (m, 2H).

¹³C NMR (100 MHz, D₂O) δ 176.04, 170.15, 53.51, 52.03, 29.30, 24.81.

4-benzyl 1-methyl (*tert*-butoxycarbonyl)-L-aspartate (**16**)



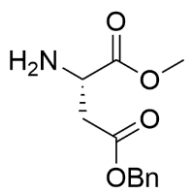
500 mg of *N*-Boc-aspartic acid β-benzyl ester (**15**) (1.55 mmol, 1.0 eq), 356 of EDC hydrochloride (1.86 mmol, 1.2 eq) and 19 mg of DMAP (0.16 mmol, 0.1 eq) were dissolved in 8 mL of anhydrous dichloromethane. 0.19 mL of anhydrous MeOH (4.65 mmol, 3.0 eq) was added and the mixture was stirred at RT overnight for 16 hours. Afterwards, the mixture was diluted with 50 mL of ethyl acetate, washed with 10% aqueous KHSO₄ (3 x 50 mL), brine (1 x 50 mL), dried over anhydrous MgSO₄, filtered, evaporated and dried *in vacuo*, which yielded 462 mg (89 %) of compound **16** as a colorless oil.

UPLC/MS – R_t = 4.590 min, ESI+ [M-Boc+H]⁺ = 238.197

¹H NMR (400 MHz, CDCl₃) δ 7.34 – 7.21 (m, 5H), 5.42 (d, *J* = 8.7 Hz, 1H), 5.06 (dd, *J* = 12.1, 3.4 Hz, 2H), 4.51 (dd, *J* = 8.8, 4.5 Hz, 1H), 3.63 (s, 3H), 2.97 (dd, *J* = 17.0, 4.7 Hz, 1H), 2.80 (dd, *J* = 17.0, 4.8 Hz, 1H), 1.37 (s, 9H).

¹³C NMR (100 MHz, CDCl₃) δ 171.47, 170.74, 155.32, 135.37, 128.61, 128.43, 128.32, 80.11, 66.78, 52.67, 49.98, 36.85, 28.30.

4-benzyl 1-methyl L-aspartate (17)



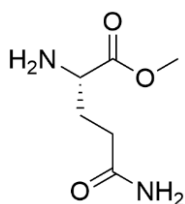
216 mg of compound **16** (0.64 mmol, 1.0 eq) was dissolved in 1 mL of anhydrous dichloromethane. 1 mL of TFA was added and the mixture was stirred at RT for 1 hour. Upon complete conversion (UPLC/MS), the mixture was evaporated and dried *in vacuo*, which yielded 220 mg (98 %) of compound **17** TFA salt as a colorless oil.

UPLC/MS – $R_t = 2.968$ min, ESI+ $[M+H]^+ = 238.201$

^1H NMR (400 MHz, CDCl_3) δ 8.10 (s, 3H), 7.34 – 7.21 (m, 5H), 5.08 (s, 2H), 4.34 (t, $J = 5.1$ Hz, 1H), 3.69 (s, 3H), 3.12 (d, $J = 5.1$ Hz, 2H).

^{13}C NMR (100 MHz, CDCl_3) δ 170.56, 168.01, 134.41, 128.70, 128.50, 68.10, 67.46, 53.96, 49.92, 33.07.

Methyl L-glutamate (19)



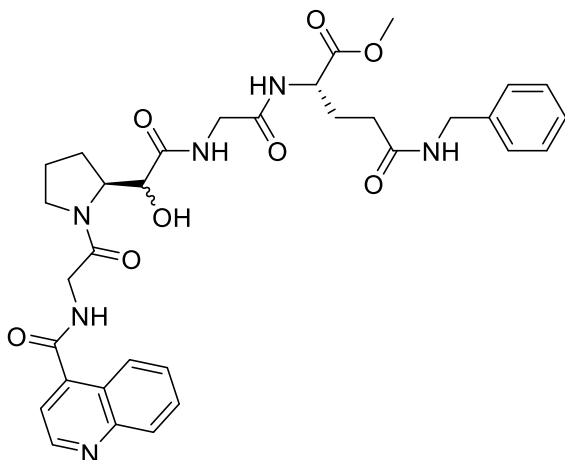
109 mg of compound **18** (0.37 mmol, 1.0 eq) were dissolved in 5 mL of methanol and a catalytical amount of $\text{Pd}(\text{OH})_2/\text{C}$ was added. The reaction mixture was stirred at RT overnight for 16 hours under hydrogen gas, after which complete hydrogenolysis of compound **18** was observed (UPLC/MS). The reaction mixture was filtered through a syringe filter, evaporated and dried *in vacuo*, which yielded 58 mg (98 %) of compound **19** as a colorless oil.

UPLC/MS – $R_t = 0.548$ min, ESI+ $[M+H]^+ = 161.224$

^1H NMR (400 MHz, D_2O) δ 3.76 (s, 3H), 3.58 (t, $J = 6.5$ Hz, 1H), 2.10 – 1.99 (m, 2H), 1.98 – 1.85 (m, 2H).

^{13}C NMR (100 MHz, D_2O) δ 177.54, 174.09, 54.11, 48.81, 30.81, 26.25.

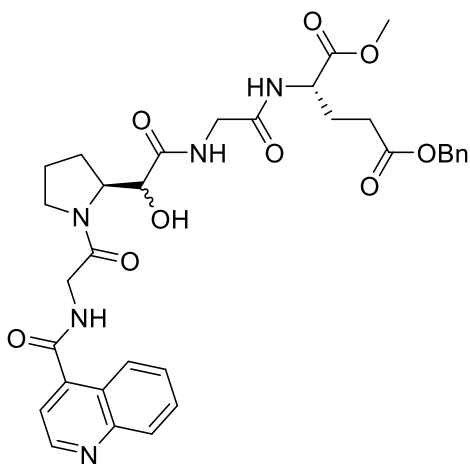
Methyl *N*⁵-benzyl-*N*²-((2-hydroxy-2-((*S*)-1-((quinoline-4-carbonyl)glycyl)pyrrolidin-2-yl)acetyl)glycyl)-L-glutamate (20a)



36 mg (47 %) of compound **20a** were prepared from 50 mg of carboxylic acid **7** by General procedure 1 (gradient 0 → 50 % acetonitrile) as a light brown amorphous solid.

UPLC/MS – $R_t = 3.276$ min, ESI+ $[M+H]^+ = 647.398$

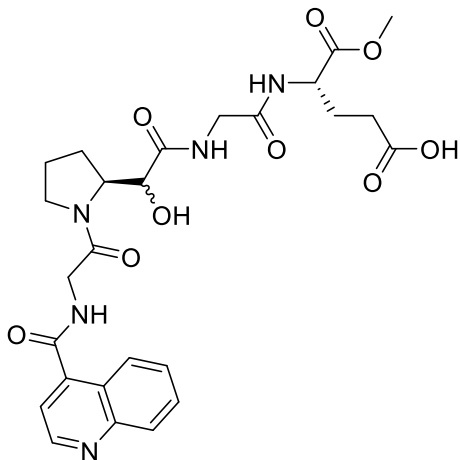
5-benzyl 1-methyl (2-hydroxy-2-((*S*)-1-((quinoline-4-carbonyl)glycyl)pyrrolidin-2-yl)acetyl)glycyl-L-glutamate (20b)



59 mg (76 %) of compound **20b** were prepared from 50 mg of carboxylic acid **7** by General procedure 1 (gradient 0 → 60 % acetonitrile) as a light brown amorphous solid.

UPLC/MS – $R_{t1} = 3.585$ min, $R_{t2} = 3.627$ min, ESI+ $[M+H]^+ = 648.380$

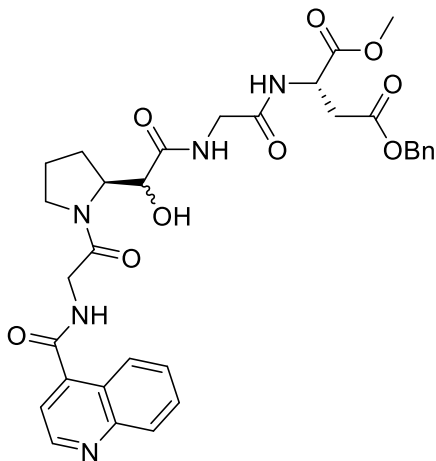
(S)-4-(2-(2-hydroxy-2-((S)-1-((quinoline-4-carbonyl)glycyl)pyrrolidin-2-yl)acetamido)acetamido)-5-methoxy-5-oxopentanoic acid (20c)



32 mg (53 %) of compound **20c** were prepared from 45 mg of carboxylic acid **7** by General procedure 1 (gradient 0 → 50 % acetonitrile) as a light brown amorphous solid.

UPLC/MS – $R_{t1} = 2.748$ min, $R_{t2} = 2.789$ min, ESI+ $[M+H]^+ = 558.356$

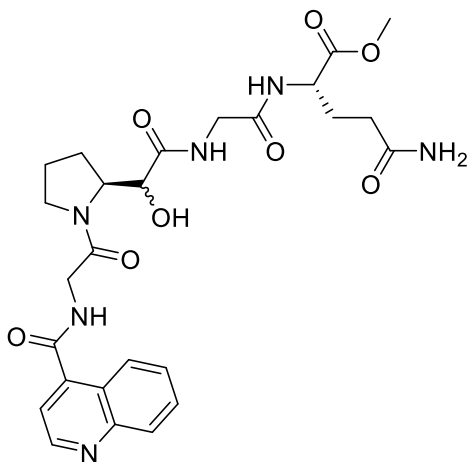
4-benzyl 1-methyl (2-hydroxy-2-((S)-1-((quinoline-4-carbonyl)glycyl)pyrrolidin-2-yl)acetyl)glycyl-L-aspartate (20d)



28 mg (41 %) of compound **20d** were prepared from 45 mg of carboxylic acid **7** by General procedure 1 (gradient 0 → 60 % acetonitrile) as a light brown amorphous solid.

UPLC/MS – $R_{t1} = 3.417$ min, $R_{t2} = 3.463$ min, ESI+ $[M+H]^+ = 634.423$

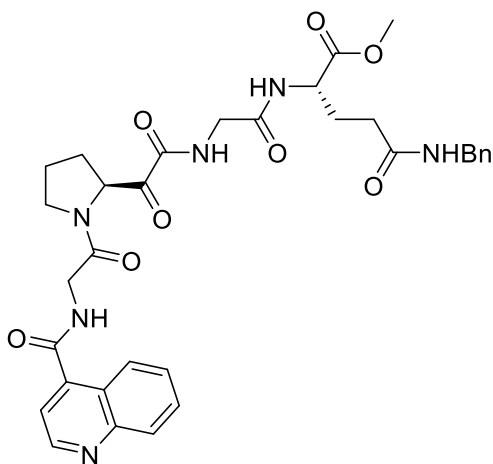
Methyl (2-hydroxy-2-((S)-1-((quinoline-4-carbonyl)glycyl)pyrrolidin-2-yl)acetyl)glycyl-L-glutamate (20e)



49 mg (54 %) of compound **20e** were prepared from 67 mg of carboxylic acid **7** by General procedure 1 (gradient 0 → 40 % acetonitrile) as a light brown amorphous solid.

UPLC/MS – $R_{t1} = 2.598$ min, $R_{t2} = 2.643$ min, ESI+ $[M+H]^+ = 557.325$

Methyl *N*⁵-benzyl-*N*²-((2-oxo-2-((S)-1-((quinoline-4-carbonyl)glycyl)pyrrolidin-2-yl)acetyl)glycyl)-L-glutamate (21a)



9 mg (isol. yield 25 %) of compound **21a** were prepared from 36 mg of α -hydroxyamide **20a** by General procedure 2 (HPLC gradient 0 → 50 % acetonitrile) as a light brown amorphous solid.

UPLC/MS – $R_t = 3.16$ - 3.39 min, ESI+ $[M+H]^+ = 645.444$

¹H NMR (500 MHz, DMSO-*d*₆): δ 9.00 (m, 1H, NH-2'); 9.00 (d, 1H, $J_{2,3} = 4.4$ Hz, H-2); 8.75 (bt, 1H, $J_{NH,CH_2} = 6.2$ Hz, COCONH); 8.46 (d, 1H, $J_{NH,CH} = 7.5$ Hz, NHCHCH₂CH₂); 8.33 (bdd, 1H, $J_{5,6} = 8.5$ Hz, $J_{5,7} = 1.5$ Hz, H-5); 8.33 (m, 1H, NHCH₂Bn); 8.09 (dm, 1H, $J_{8,7} = 8.4$ Hz, H-8); 7.84 (ddd, 1H, $J_{7,8} = 8.4$ Hz, $J_{8,7} = 6.9$ Hz, $J_{7,5} = 1.4$ Hz, H-7); 7.69 (ddd, 1H, $J_{6,5} = 8.5$ Hz, $J_{6,7} = 6.9$ Hz, $J_{6,8} = 1.3$ Hz, H-6); 7.58 (d, 1H, $J_{3,2} = 4.4$ Hz, H-3); 7.34 – 7.27 (m, 2H, H-*m*-Bn); 7.25 – 7.18 (m, 3H, H-*o,p*-Bn); 5.24 (dd, 1H, $J_{1',2''} = 9.2$ and 4.0 Hz, H-1'); 4.30 – 4.18 (m, 3H, NHCHCH₂CH₂, CH₂-Bn); 4.28 (dd, 1H, $J_{gem} = 16.6$ Hz, $J_{2'b,NH} = 5.8$ Hz, H-2'b); 4.16 (dd, 1H, $J_{gem} = 16.8$ Hz, $J_{2'a,NH} = 5.9$ Hz, H-2'a); 3.88 – 3.78 (m, 2H, NHCH₂CONH); 3.70 – 3.58 (m, 2H, H-4'); 3.62 (s, 3H, COOCH₃); 2.27 – 2.15 (m, 3H, H-2''b, NHCHCH₂CH₂); 2.03 – 1.72 (m, 5H, H-3'', 2''a, NHCHCH₂CH₂).

¹³C NMR (125.7 MHz, DMSO-*d*₆): δ 194.83 (COCONH); 172.43 (COOCH₃); 171.28 (CHCH₂CH₂CONH); 168.13 (CH₂CONHCH); 167.06 (CO-1'); 166.57 (CO-3'); 160.46 (COCONH); 150.06 (CH-2); 147.27 (C-8a); 143.12 (C-4); 139.70 (C-*i*-Bn); 130.45 (CH-7); 128.74 (CH-8); 128.47 (CH-*m*-Bn); 127.73 (CH-6); 127.39 (CH-*o*-Bn); 126.93 (CH-*p*-Bn); 126.14 (CH-5); 124.49 (C-4a); 119.31 (CH-3); 60.38 (CH-1'); 52.13 (COOCH₃); 51.80 (NHCHCH₂CH₂); 46.08 (CH₂-4'); 42.24 (CH₂-Bn); 41.74 (NHCH₂CONH); 41.55 (CH₂-2'); 31.50 (NHCHCH₂CH₂); 27.66 (CH₂-2''); 27.10 (NHCHCH₂CH₂); 24.66 (CH₂-3'').

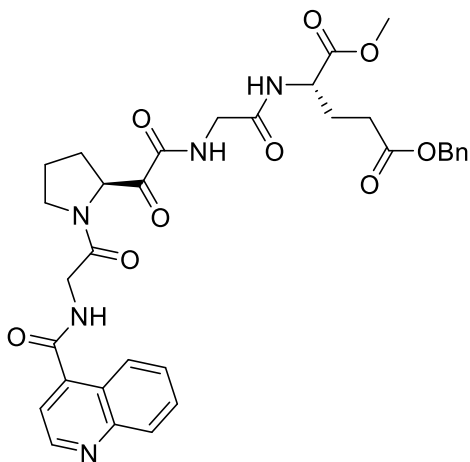
HRMS – C₃₃H₃₆N₆NaO₈ [M+Na]⁺ calcd. 667.24868, found 667.24817

Optical rotation – $[\alpha]_{589}^{20} = -26.8^\circ$

IR [cm⁻¹] – 3200(m), 3061 (w), 2952 (m), 2883 (m), 1739 (m), 1668 (s), 1585 (m), 1539 (m), 1507 (s), 1453 (s), 1379 (m), 1248 (m), 1203 (m), 1177 (m).

Elemental analysis – calcd. % (found %): C – 55.41 (50.16); H – 4.92 (5.23); N – 11.08 (9.61); F – *insufficient material*.

5-benzyl 1-methyl (2-oxo-2-((S)-1-((quinoline-4-carbonyl)glycyl)pyrrolidin-2-yl)acetyl)glycyl-L-glutamate (21b)



19 mg (isol. yield 50 %) of compound **21b** were prepared from 38 mg of α -hydroxyamide **20b** by General procedure 2 (HPLC gradient 0 \rightarrow 50 % acetonitrile) as a light brown amorphous solid.

UPLC/MS – R_t = 3.51-3.76 min, ESI+ $[M+H]^+$ = 646.395

1H NMR (500 MHz, DMSO- d_6): δ 8.99 (d, 1H, $J_{2,3}$ = 4.4 Hz, H-2); 8.97 (m, 1H, NH-2'); 8.78 (bt, 1H, J_{NH,CH_2} = 6.0 Hz, COCONH); 8.42 (d, 1H, $J_{NH,CH}$ = 7.7 Hz, NHCHCH₂CH₂); 8.32 (dm, 1H, $J_{5,6}$ = 8.5 Hz, H-5); 8.08 (dm, 1H, $J_{8,7}$ = 8.5 Hz, H-8); 7.82 (ddd, 1H, $J_{7,8}$ = 8.5 Hz, $J_{8,7}$ = 6.9 Hz, $J_{7,5}$ = 1.4 Hz, H-7); 7.68 (ddd, 1H, $J_{6,5}$ = 8.5 Hz, $J_{6,7}$ = 6.9 Hz, $J_{6,8}$ = 1.3 Hz, H-6); 7.57 (d, 1H, $J_{3,2}$ = 4.4 Hz, H-3); 7.41 – 7.29 (m, 5H, H-*o,m,p*-Bn); 5.23 (dd, 1H, $J_{1',2''}$ = 9.3 and 4.0 Hz, H-1''); 5.13 – 5.03 (m, 2H, CH₂-Bn); 4.34 (ddd, 1H, J_{CH,CH_2} = 9.3 Hz, $J_{CH,NH}$ = 7.7 Hz, J_{CH,CH_2} = 5.2 Hz, NHCHCH₂CH₂); 4.27 (dd, 1H, J_{gem} = 16.8 Hz, $J_{2'b,NH}$ = 6.1 Hz, H-2'b); 4.15 (dd, 1H, J_{gem} = 16.8 Hz, $J_{2'a,NH}$ = 5.9 Hz, H-2'a); 3.86 – 3.75 (m, 2H, NHCH₂CONH); 3.70 – 3.60 (m, 2H, H-4''); 3.62 (s, 3H, COOCH₃); 2.46 – 2.41 (m, 2H, NHCHCH₂CH₂); 2.20 (m, 1H, H-2'b); 2.07 – 1.73 (m, 5H, H-3'',2''a, NHCHCH₂CH₂).

^{13}C NMR (125.7 MHz, DMSO- d_6): δ 194.75 (COCONH); 172.22 (COOCH₃); 172.18 (CHCH₂CH₂CO); 168.18 (CH₂CONHCH); 167.11 (CO-1'); 166.56 (CO-3'); 160.50 (COCONH); 150.19 (CH-2); 147.56 (C-8a); 142.84 (C-4); 136.31 (C-*i*-Bn); 130.28 (CH-7); 128.98 (CH-8); 128.64 (CH-*m*-Bn); 128.22 (CH-*p*-Bn); 128.15 (CH-*o*-Bn); 127.62 (CH-6); 126.10 (CH-5); 124.45 (C-4a); 119.28 (CH-3); 65.75 (CH₂-Bn); 60.41 (CH-1''); 52.20

(COOCH₃); 51.26 (NHCHCH₂CH₂); 46.07 (CH₂-4''); 41.83 (NHCH₂CONH); 41.54 (CH₂-2'); 29.90 (NHCHCH₂CH₂); 27.60 (CH₂-2''); 26.29 (NHCHCH₂CH₂); 24.63 (CH₂-3'').

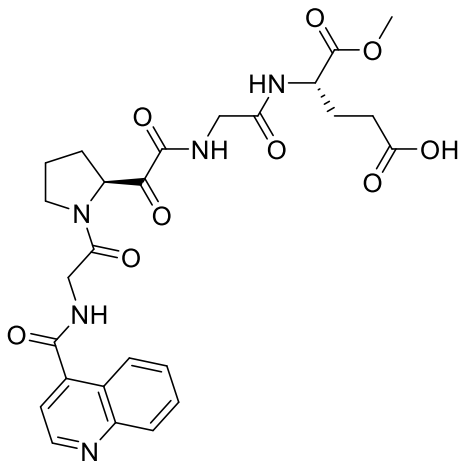
HRMS – C₃₃H₃₅N₅NaO₉ [M+Na]⁺ calcd. 668.23270, found 668.23204

Optical rotation – [α]₅₈₉²⁰ = -27.1 °

IR [cm⁻¹] – 3200 (m), 3061 (w), 3036 (w), 2953 (m), 2918 (s), 2886 (m), 1735 (m), 1671 (s), 1585 (m), 1533 (m), 1507 (s), 1454 (s), 1381 (m), 1250 (m), 1203 (m), 1173 (m).

Elemental analysis – calcd. % (found %): C – 55.34 (53.89); H – 4.78 (5.27); N – 9.22 (8.67); F – 7.50 (3.93).

(S)-5-methoxy-5-oxo-4-(2-(2-oxo-2-((S)-1-((quinoline-4-carbonyl)glycyl)pyrrolidin-2-yl)acetamido)acetamido)pentanoic acid (21c)



20 mg (isol. yield 63 %) of compound **21c** were prepared from 32 mg of α -hydroxyamide **20c** by General procedure 2 (HPLC gradient 0 → 50 % acetonitrile) as a light brown amorphous solid.

UPLC/MS – R_t = 2.68-2.84 min, ESI+ [M+H]⁺ = 556.326

¹H NMR (500 MHz, DMSO-d₆): δ 8.99 (m, 1H, NH-2'); 8.99 (d, 1H, $J_{2,3}$ = 4.4 Hz, H-2); 8.77 (t, 1H, $J_{NH,CH2}$ = 6.1 Hz, COCONH); 8.41 (d, 1H, $J_{NH,CH}$ = 7.6 Hz, NHCHCH₂CH₂); 8.33 (bdd, 1H, $J_{5,6}$ = 8.5 Hz, $J_{5,7}$ = 1.5 Hz, H-5); 8.09 (dm, 1H, $J_{8,7}$ = 8.5 Hz, H-8); 7.83 (ddd, 1H, $J_{7,8}$ = 8.5 Hz, $J_{8,7}$ = 6.9 Hz, $J_{7,5}$ = 1.5 Hz, H-7); 7.69 (ddd, 1H, $J_{6,5}$ = 8.4 Hz, $J_{6,7}$ = 6.9 Hz, $J_{6,8}$ = 1.3 Hz, H-6); 7.57 (d, 1H, $J_{3,2}$ = 4.4 Hz, H-3); 5.24 (dd, 1H, $J_{1'',2''}$ = 9.3 and 4.1 Hz, H-1''); 4.31 (ddd, 1H, $J_{CH,CH2}$ = 9.2 Hz, $J_{CH,NH}$ = 7.6 Hz, $J_{CH,CH2}$ = 5.3 Hz, NHCHCH₂CH₂); 4.28 (dd, 1H, J_{gem} = 16.8 Hz, $J_{2'b,NH}$ = 6.1 Hz, H-2'b); 4.16 (dd, 1H, J_{gem} =

16.8 Hz, $J_{2'a,NH} = 5.8$ Hz, H-2'a); 3.87 – 3.76 (m, 2H, NHCH₂CONH); 3.69 – 3.57 (m, 2H, H-4''); 3.63 (s, 3H, COOCH₃); 2.35 – 2.20 (m, 3H, NHCHCH₂CH₂, H-2''b); 2.06 – 1.83 (m, 4H, H-3'', 2''a, NHCHCH₂CH₂-b); 1.80 (m, 1H, NHCHCH₂CH₂-a).

¹³C NMR (125.7 MHz, DMSO-d₆): δ 194.81 (COCONH); 173.85 (COOH); 172.47 (COOCH₃); 168.18 (CH₂CONHCH); 167.11 (CO-1'); 166.58 (CO-3'); 160.49 (COCONH); 150.17 (CH-2); 147.50 (C-8a); 142.93 (C-4); 130.34 (CH-7); 128.93 (CH-8); 127.67 (CH-6); 126.12 (CH-5); 124.47 (C-4a); 119.30 (CH-3); 60.43 (CH-1'); 52.16 (COOCH₃); 51.37 (NHCHCH₂CH₂); 46.09 (CH₂-4''); 41.77 (NHCH₂CONH); 41.55 (CH₂-2'); 29.93 (NHCHCH₂CH₂); 27.66 (CH₂-2''); 26.41 (NHCHCH₂CH₂); 24.66 (CH₂-3').

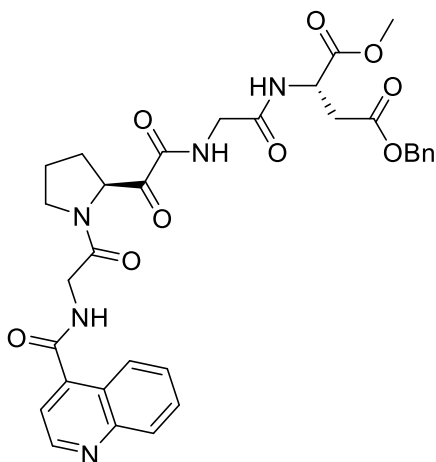
HRMS – C₂₆H₃₀N₅O₉ [M+H]⁺ calcd. 556.20380, found 556.20384

Optical rotation – $[\alpha]_{589}^{20} = -15.7^\circ$

IR [cm⁻¹] – 3354 (s), 3200 (m), 3061 (w), 3013 (w), 2955 (m), 2918 (s), 2850 (m), 1734 (m), 1717 (m), 1668 (s), 1586 (m), 1539 (m), 1507 (s), 1467 (s), 1378 (m), 1256 (m), 1202 (m), 1178 (m).

Elemental analysis – *insufficient material*

4-benzyl 1-methyl (2-oxo-2-((S)-1-((quinoline-4-carbonyl)glycyl)pyrrolidin-2-yl)acetyl)glycyl-L-aspartate (21d)



15 mg (isol. yield 54 %) of compound **21d** were prepared from 28 mg of α -hydroxyamide **20d** by General procedure 2 (HPLC gradient 0 → 50 % acetonitrile) as a light brown amorphous solid.

UPLC/MS – R_t = 3.30-3.57 min, ESI+ [M+H]⁺ = 632.414

¹H NMR (500 MHz, DMSO-d₆): δ 9.02 (d, 1H, $J_{2,3} = 4.4$ Hz, H-2); 9.01 (m, 1H, NH-2'); 8.78 (t, 1H, $J_{NH,CH_2} = 6.2$ Hz, COCONH); 8.55 (d, 1H, $J_{NH,CH} = 8.0$ Hz, NHCHCH₂); 8.34 (dd, 1H, $J_{5,6} = 8.5$ Hz, $J_{5,7} = 1.6$ Hz, H-5); 8.10 (dm, 1H, $J_{8,7} = 8.5$ Hz, H-8); 7.84 (ddd, 1H, $J_{7,8} = 8.5$ Hz, $J_{8,7} = 6.9$ Hz, $J_{7,5} = 1.4$ Hz, H-7); 7.70 (ddd, 1H, $J_{6,5} = 8.5$ Hz, $J_{6,7} = 6.9$ Hz, $J_{6,8} = 1.2$ Hz, H-6); 7.60 (d, 1H, $J_{3,2} = 4.4$ Hz, H-3); 7.41 – 7.27 (m, 5H, H-*o,m,p*-Bn); 5.24 (dd, 1H, $J_{1'',2''} = 9.2$ and 4.2 Hz, H-1''); 5.16 – 5.07 (m, 2H, CH₂-Bn); 4.71 (m, 1H, NHCHCH₂); 4.28 (dd, 1H, $J_{gem} = 16.8$ Hz, $J_{2'b,NH} = 6.1$ Hz, H-2'b); 4.16 (dd, 1H, $J_{gem} = 16.7$ Hz, $J_{2'a,NH} = 5.9$ Hz, H-2'a); 3.88 – 3.75 (m, 2H, NHCH₂CONH); 3.72 – 3.62 (m, 2H, H-4''); 3.60 (s, 3H, COOCH₃); 2.92 – 2.71 (m, 2H, NHCHCH₂); 2.23 (m, 1H, H-2''b); 2.00 (m, 1H, H-3''b); 1.92 – 1.81 (m, 2H, H-2''a, 3''a).

¹³C NMR (125.7 MHz, DMSO-d₆): δ 194.86 (COCONH); 171.15 (COOCH₃); 170.00 (CHCH₂CO); 168.01 (CH₂CONHCH); 167.01 (CO-1'); 166.57 (CO-3'); 160.48 (COCONH); 149.98 (CH-2); 147.07 (C-8a); 143.32 (C-4); 136.06 (C-*i*-Bn); 130.55 (CH-7); 129.11 (CH-8); 128.65 (CH-*m*-Bn); 128.28 (CH-*p*-Bn); 128.18 (CH-*o*-Bn); 127.80 (CH-6); 126.17 (CH-5); 124.52 (C-4a); 119.34 (CH-3); 66.11 (CH₂-Bn); 60.43 (CH-1''); 52.44 (COOCH₃); 48.68 (NHCHCH₂); 46.08 (CH₂-4''); 41.76 (NHCH₂CONH); 41.56 (CH₂-2'); 36.06 (NHCHCH₂); 27.68 (CH₂-2''); 24.66 (CH₂-3'').

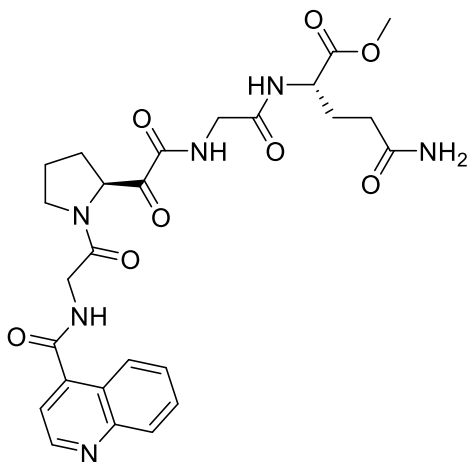
HRMS – C₃₂H₃₄N₅O₉ [M+H]⁺ calcd. 632.23510, found 632.23533

Optical rotation – $[\alpha]_{589}^{20} = -19.9^\circ$

IR [cm⁻¹] – 3200 (m), 3061 (w), 3036 (w), 2952 (m), 2883 (m), 1737 (m), 1670 (s), 1585 (m), 1531 (m), 1507 (s), 1456 (s), 1382 (m), 1248 (m), 1204 (m), 1174 (m).

Elemental analysis – calcd. % (found %): C – 54.77 (52.15); H – 4.60 (5.30); N – 9.39 (8.24); F – *insufficient material*.

Methyl (2-oxo-2-((S)-1-((quinoline-4-carbonyl)glycyl)pyrrolidin-2-yl)acetyl)glycyl-L-glutamate (21e)



10 mg (isol. yield 20 %) of compound **21e** were prepared from 49 mg of α -hydroxyamide **20e** by General procedure 2 (HPLC gradient 0 \rightarrow 50 % acetonitrile) as a light brown amorphous solid.

UPLC/MS – $R_t = 2.53$ - 2.71 min, ESI+ $[M+H]^+ = 555.331$

1H NMR (500 MHz, DMSO- d_6): δ 9.00 (m, 1H, NH-2'); 9.00 (d, 1H, $J_{2,3} = 4.4$ Hz, H-2); 8.75 (t, 1H, $J_{NH,CH_2} = 6.0$ Hz, COCONH); 8.44 (d, 1H, $J_{NH,CH} = 7.5$ Hz, NHCHCH₂CH₂); 8.32 (bdd, 1H, $J_{5,6} = 8.5$ Hz, $J_{5,7} = 1.4$ Hz, H-5); 8.09 (dm, 1H, $J_{8,7} = 8.4$ Hz, H-8); 7.83 (ddd, 1H, $J_{7,8} = 8.4$ Hz, $J_{8,7} = 6.9$ Hz, $J_{7,5} = 1.4$ Hz, H-7); 7.69 (ddd, 1H, $J_{6,5} = 8.3$ Hz, $J_{6,7} = 6.9$ Hz, $J_{6,8} = 1.3$ Hz, H-6); 7.57 (d, 1H, $J_{3,2} = 4.4$ Hz, H-3); 7.28 (bs, 1H, NH₂-b); 6.79 (bs, 1H, NH₂-a); 5.24 (dd, 1H, $J_{1'',2''} = 9.2$ and 4.1 Hz, H-1''); 4.28 (dd, 1H, $J_{gem} = 16.8$ Hz, $J_{2'b,NH} = 6.2$ Hz, H-2'b); 4.25 (ddd, 1H, $J_{CH,CH_2} = 9.0$ Hz, $J_{CH,NH} = 7.4$ Hz, $J_{CH,CH_2} = 5.4$ Hz, NHCHCH₂CH₂); 4.16 (dd, 1H, $J_{gem} = 16.8$ Hz, $J_{2'a,NH} = 5.9$ Hz, H-2'a); 3.85 – 3.77 (m, 2H, NHCH₂CONH); 3.71 – 3.62 (m, 2H, H-4'); 3.62 (s, 3H, COOCH₃); 2.23 (m, 1H, H-2''b); 2.16 – 2.06 (m, 2H, NHCHCH₂CH₂); 2.01 (m, 1H, H-3''b); 1.98 – 1.83 (m, 3H, H-3''a, 2''a, NHCHCH₂CH₂-b); 1.78 (m, 1H, NHCHCH₂CH₂-a).

^{13}C NMR (125.7 MHz, DMSO- d_6): δ 194.82 (COCONH); 173.43 (CONH₂); 172.48 (COOCH₃); 168.12 (CH₂CONHCH); 167.10 (CO-1'); 166.58 (CO-3'); 160.46 (COCONH); 150.14 (CH-2); 147.48 (C-8a); 142.95 (C-4); 130.36 (CH-7); 128.89 (CH-8); 127.68 (CH-6); 126.12 (CH-5); 124.47 (C-4a); 119.30 (CH-3); 60.39 (CH-1''); 52.10 (COOCH₃); 51.80 (NHCHCH₂CH₂); 46.09 (CH₂-4'); 41.72 (NHCH₂CONH); 41.54 (CH₂-2'); 31.16 (NHCHCH₂CH₂); 27.68 (CH₂-2''); 26.86 (NHCHCH₂CH₂); 24.67 (CH₂-3').

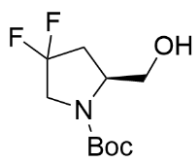
HRMS – C₂₆H₃₁N₆O₈ [M+H]⁺ calcd. 555.21979, found 555.21963

Optical rotation – $[\alpha]_{589}^{20} = -16.1^\circ$

IR [cm⁻¹] – 3200 (m), 3061 (w), 2963 (m) 2932 (m), 1738 (m), 1668 (s), 1585 (m), 1539 (m), 1507 (m), 1247 (m), 1202 (m).

Elemental analysis – *insufficient material*

***Tert*-butyl (S)-4,4-difluoro-2-(hydroxymethyl)pyrrolidine-1-carboxylate (23)**



143 mg of LiAlH₄ (3.77 mmol, 1.0 eq) was dissolved in 5 mL of anhydrous tetrahydrofuran and cooled down to 0 °C under an argon atmosphere.

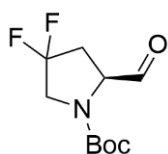
To this solution, 1.00 g of *N*-Boc-4,4-difluoro-L-proline methyl ester (**22**) (3.77 mmol, 1.0 eq) in 5 mL of anhydrous tetrahydrofuran was added dropwise. The mixture was stirred for 1 hour and warmed up to RT, after which it was filtered through a Celite plug, washed with ethyl acetate and the filtrate was neutralized to pH 7 by dropwise addition of 1M HCl in ethyl acetate. It was then concentrated under reduced pressure and purified on a silica column (mobile phase cyclohexane/ethyl acetate = 3/2; TLC in cyclohexane/ethyl acetate = 1/1, R_f = 0.57). Corresponding fractions were pooled and evaporated, yielding 586 mg (66 %) of alcohol **23** as a colorless oil.

UPLC/MS – R_t = 3.772 min, ESI+ [M-Boc+H]⁺ = 138.066

¹H NMR (400 MHz, CDCl₃) δ 4.16 (s, 1H), 3.93 – 3.56 (m, 1H), 3.74 – 3.67 (m, 2H), 3.63 (q, *J* = 12.8 Hz, 1H), 3.54 – 3.26 (m, 1H), 2.57 – 2.40 (m, 1H), 2.14 (s, 1H), 1.47 (s, 9H).

¹³C NMR (100 MHz, CDCl₃) δ 155.88, 126.16, 81.64, 65.94, 58.54, 54.02, 36.63, 28.31.

***Tert*-butyl (S)-4,4-difluoro-2-formylpyrrolidine-1-carboxylate (24)**



534 mg of alcohol **23** (2.25 mmol, 1.0 eq) was dissolved in 10 mL of ethyl acetate. 950 mg of IBX (3.38 mmol, 1.5 eq) were added and the suspension was refluxed at 90 °C for 3 hours. Upon full conversion (monitored by TLC),

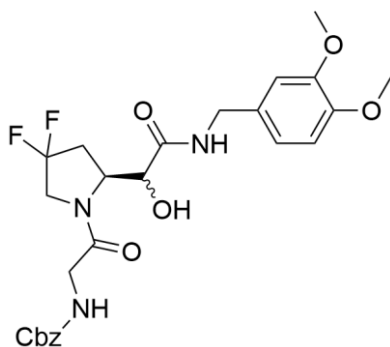
the suspension was cooled down to RT and filtered. The filtrate was concentrated under reduced pressure and purified on a silica column (mobile phase cyclohexane/ethyl acetate = 3/1, TLC in cyclohexane/ethyl acetate = 2/1, R_f = 0.44), which yielded 418 mg (79 %) of aldehyde **24** as a colorless oil.

UPLC/MS – R_t = 3.527 min, ESI+ [M-Boc+H]⁺ = 136.035

¹H NMR (400 MHz, CDCl₃) δ 9.57 (d, *J* = 24.1 Hz, 1H), 4.47 – 4.21 (m, 1H), 3.92 – 3.70 (m, 2H), 2.69 – 2.37 (m, 2H), 1.49 – 1.43 (m, 9H).

¹³C NMR (100 MHz, CDCl₃) δ 198.33, 157.16, 106.93, 82.09, 62.19, 53.42, 36.02, 28.25.

Benzyl (*S*)-(2-(2-(2-((3,4-dimethoxybenzyl)amino)-1-hydroxy-2-oxoethyl)-4,4-difluoropyrrolidin-1-yl)-2-oxoethyl)carbamate (26)



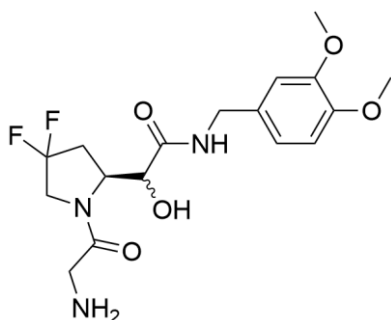
50 mg of aldehyde **24** (0.21 mmol, 1.0 eq), 38 mg of 3,4-dimethoxybenzyl isocyanide (**25**) (0.21 mmol, 1.0 eq) and 45 mg of *N*-benzyloxycarbonylglycine (**2**) (0.21 mmol, 1.0 eq) were dissolved in 5 mL of anhydrous dichloromethane and stirred at RT for 2 hours. Afterwards, 1 mL of TFA was added and the mixture was stirred for 1 hour at RT. Volatiles were evaporated *in vacuo*, the solids were redissolved in 5 mL of anhydrous dichloromethane and were cooled to 0 °C on an ice bath, after which 2 mL of TEA were added dropwise. The mixture was allowed to reach RT and was stirred for 16 hours. The reaction course was monitored by UPLC/MS. After full conversion, the mixture was diluted with 40 mL of dichloromethane, washed twice with saturated NaHCO₃ (50 mL) and twice with H₂O (50 mL). The organic phase was dried with anhydrous MgSO₄, filtered and evaporated to dryness, which yielded 72 mg (65 %) of compound **26** as a brown oil.

UPLC/MS – R_{t1} = 3.567 min, R_{t2} = 3.602 min, ESI+ [M+H]⁺ = 522.233

¹H NMR (400 MHz, CDCl₃) δ 8.18 (dt, *J* = 1.8, 0.8 Hz, 1H), 7.34 – 7.25 (m, 5H), 6.77 (d, *J* = 14.1 Hz, 3H), 6.17 (s, 1H), 5.76 (dt, *J* = 8.5, 4.5 Hz, 1H), 5.05 (dd, *J* = 4.8, 1.8 Hz, 1H), 4.65 – 4.45 (m, 1H), 4.41 – 4.31 (m, 2H), 4.30 – 4.15 (m, 2H), 3.82 (s, 3H), 3.81 (s, 3H), 3.79 (d, *J* = 3.6 Hz, 2H), 2.80 – 2.59 (m, 1H), 2.51 – 2.36 (m, 1H), 2.01 (s, 2H).

¹³C NMR (100 MHz, CDCl₃) δ 170.98, 170.82, 169.67, 149.07, 148.50, 136.14, 130.59, 128.53, 128.24, 128.04, 120.10, 111.21, 111.19, 111.12, 67.15, 60.41, 55.92, 55.88, 43.02, 42.68, 41.97, 35.11, 21.04.

(S)-2-(4,4-difluoro-1-glycylpyrrolidin-2-yl)-N-(3,4-dimethoxybenzyl)-2-hydroxyacetamide (27)



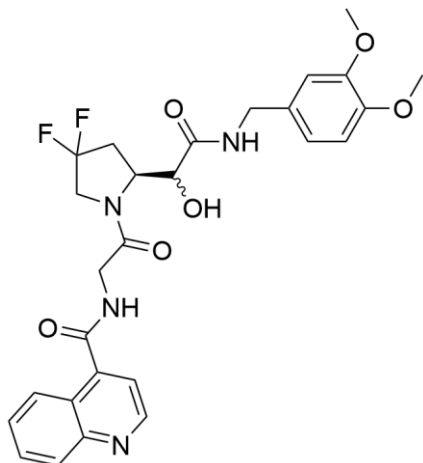
72 mg of compound **26** (0.14 mmol, 1.0 eq) were dissolved in 5 mL of methanol. A catalytical amount of Pd(OH)₂/C was added and the suspension was stirred at RT under a hydrogen atmosphere for 16 hours. The suspension was filtered using a syringe filter and the volatiles were evaporated *in vacuo*. The crude mixture was then purified by reversed-phase HPLC using a 0 → 40 % gradient from 0.1 % TFA (aq.) to acetonitrile. Corresponding fractions were pooled and lyophilized, yielding 35 mg (51 %) of compound **27** TFA salt as a light brown amorphous solid.

UPLC/MS – R_{t1} = 2.783 min, R_{t2} = 2.883 min, ESI+ [M+H]⁺ = 388.325

¹H NMR (400 MHz, CDCl₃) δ 8.23 (s, 3H), 6.82 – 6.66 (m, 3H), 6.05 (s, 1H), 4.84 (s, 1H), 4.52 (s, 1H), 4.40 (d, *J* = 5.8 Hz, 2H), 4.32 (d, *J* = 6.2 Hz, 2H), 3.85 (s, 6H), 3.81 (s, 1H), 3.79 (s, 1H), 3.77 (t, *J* = 2.8 Hz, 1H), 2.39 (d, *J* = 58.9 Hz, 2H).

¹³C NMR (100 MHz, CDCl₃) δ 171.55, 166.11, 149.24, 148.69, 130.06, 120.26, 116.53, 111.32, 111.22, 69.81, 68.46, 56.05, 56.01, 55.91, 45.86, 42.22, 35.07.

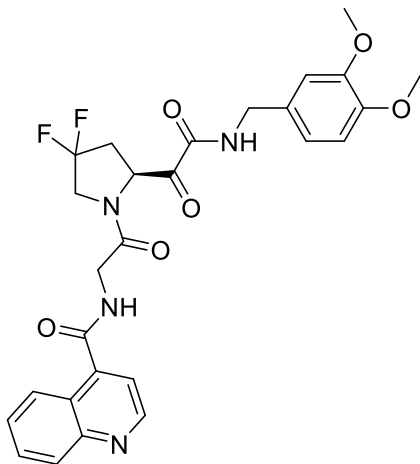
(S)-N-(2-(2-(2-((3,4-dimethoxybenzyl)amino)-1-hydroxy-2-oxoethyl)-4,4-difluoropyrrolidin-1-yl)-2-oxoethyl)quinoline-4-carboxamide (28)



15 mg (39 %) of compound **28** were prepared from 35 mg of compound **27** TFA salt using General procedure 1 (gradient 0 → 45 % acetonitrile) as a light brown amorphous solid.

UPLC/MS – R_{t1} = 3.280 min, R_{t2} = 3.377 min, ESI+ [M+H]⁺ = 543.276

(S)-N-(2-(2-(2-((3,4-dimethoxybenzyl)amino)-2-oxoacetyl)-4,4-difluoropyrrolidin-1-yl)-2-oxoethyl)quinoline-4-carboxamide (29)



11 mg (73 %) of compound **29** TFA salt were prepared from 15 mg of compound **28** using General procedure 2 (HPLC gradient 0 → 40 % acetonitrile) as a light brown amorphous solid.

UPLC/MS – $R_t = 3.24\text{--}3.52$ min, ESI+ $[M+H]^+ = 541.238$

^1H NMR (500 MHz, DMSO- d_6): 9.33 (bt, 1H, $J_{\text{NH,CH}_2} = 6.3$ Hz, COCONH); 9.07 (bt, 1H, $J_{\text{NH,CH}_2} = 6.0$ Hz, NH-2'); 9.01 (d, 1H, $J_{2,3} = 4.4$ Hz, H-2); 8.31 (bdd, 1H, $J_{5,6} = 8.4$ Hz, $J_{5,7} = 1.5$ Hz, H-5); 8.10 (dm, 1H, $J_{8,7} = 8.5$ Hz, H-8); 7.84 (ddd, 1H, $J_{7,8} = 8.4$ Hz, $J_{8,7} = 6.9$ Hz, $J_{7,5} = 1.4$ Hz, H-7); 7.67 (ddd, 1H, $J_{6,5} = 8.4$ Hz, $J_{6,7} = 6.9$ Hz, $J_{6,8} = 1.3$ Hz, H-6); 7.58 (d, 1H, $J_{3,2} = 4.4$ Hz, H-3); 6.91 (d, 1H, $J_{2,6} = 2.0$ Hz, H-2-Ph); 6.86 (d, 1H, $J_{5,6} = 8.3$ Hz, H-5-Ph); 6.80 (dd, 1H, $J_{6,5} = 8.2$ Hz, $J_{6,2} = 2.0$ Hz, H-6-Ph); 5.43 (dd, 1H, $J_{1',2''} = 10.0$ and 5.4 Hz, H-1'); 4.16 – 4.34 (m, 6H, CH₂-Ph, H-2', H-4'); 3.71 (s, 3H, CH₃O-3-Ph); 3.70 (s, 3H, CH₃O-4-Ph); 2.96 (m, 1H, H-2''b); 2.53 (m, 1H, H-2''a).

^{13}C NMR (125.7 MHz, DMSO- d_6): 192.89 (COCONH); 167.28 (CO-3'); 167.11 (CO-1'); 159.91 (COCONH); 150.06 (CH-2); 148.77 (C-3-Ph); 148.09 (C-4-Ph); 147.27 (C-8a); 142.95 (C-4); 130.94 (C-1-Ph); 130.44 (CH-7); 128.77 (CH-8); 127.72 (CH-6); 127.58 (C-3''); 126.04 (CH-5); 124.44 (C-4a); 119.80 (CH-6-Ph); 119.30 (CH-3); 111.87 and 111.75 (CH-2,5-Ph); 58.38 (CH-1'); 55.69 and 55.57 (CH₃O); 52.40 (d, $J_{\text{C,F}} = 31.7$ Hz, CH₂-4'); 42.13 (CH₂-Ph); 41.37 (CH₂-2'); 35.66 (d, $J_{\text{C,F}} = 24.5$ Hz, CH₂-2'').

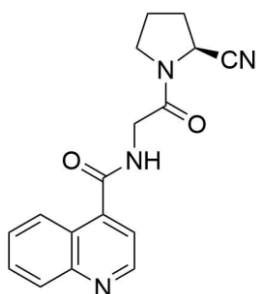
HRMS – C₂₇H₂₇O₆N₄F₂ $[M+H]^+$ calcd. 541.18932, found 541.18880

Optical rotation – $[\alpha]_{589}^{20} = -39.3^\circ$

IR [cm^{-1}] – 3061 (w), 3006 (w), 2962 (m), 2938 (m), 2837 (s), 1737 (m), 1674 (s), 1610 (m), 1593 (m), 1581 (m), 1537 (m), 1517 (s), 1369 (m), 1265 (m), 1235 (m), 1140 (s), 1026 (m).

Elemental analysis – calcd. % (found %): C – 53.22 (45.16); H – 4.16 (4.84); N – 8.56 (6.09); F – 14.51 (9.03).

(S)-N-(2-(2-cyanopyrrolidin-1-yl)-2-oxoethyl)quinoline-4-carboxamide (R1)



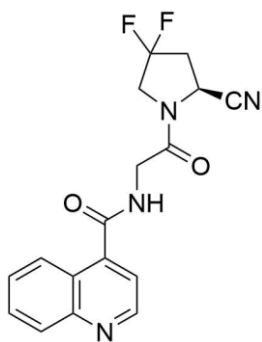
This compound was prepared according to a published procedure⁸⁰.

UPLC/MS – $R_t = 2.896$ min, ESI+ $[M+H]^+ = 309.267$

$^1\text{H NMR}$ (500 MHz, DMSO- d_6): 9.20 (bt, 1H, $J_{\text{NH},2'} = 5.9$ Hz, NH-2'); 9.11 (d, 1H, $J_{2,3} = 4.6$ Hz, H-2); 8.45 (bdd, 1H, $J_{5,6} = 8.5$ Hz, $J_{5,7} = 1.5$ Hz, H-5); 8.16 (dm, 1H, $J_{8,7} = 8.5$ Hz, H-8); 7.93 (ddd, 1H, $J_{7,8} = 8.5$ Hz, $J_{8,7} = 6.9$ Hz, $J_{7,5} = 1.5$ Hz, H-7); 7.79 (ddd, 1H, $J_{6,5} = 8.5$ Hz, $J_{6,7} = 6.9$ Hz, $J_{6,8} = 1.3$ Hz, H-6); 7.72 (d, 1H, $J_{3,2} = 4.6$ Hz, H-3); 4.86 (dd, 1H, $J_{1'',2''} = 7.4$ and 3.6 Hz, H-1''); 4.27 (dd, 1H, $J_{\text{gem}} = 16.9$ Hz, $J_{2'b,\text{NH}} = 6.2$ Hz, H-2'b); 4.21 (dd, 1H, $J_{\text{gem}} = 16.9$ Hz, $J_{2'a,\text{NH}} = 5.8$ Hz, H-2'a); 3.75 (ddd, 1H, $J_{\text{gem}} = 9.6$ Hz, $J_{4'',3''} = 7.7$ and 3.6 Hz, H-4'b); 3.55 (td, 1H, $J_{\text{gem}} = J_{4'',3''} = 9.2$ Hz, $J_{4'',3''} = 6.8$ Hz, H-4'a); 2.26 – 1.98 (m, 4H, H-2'',3'').

$^{13}\text{C NMR}$ (125.7 MHz, DMSO- d_6): 167.59 (CO-3'); 166.99 (CO-1'); 149.48 (CH-2); 145.76 (C-8a); 144.66 (C-4); 131.41 (CH-7); 128.32 (CH-6); 127.57 (CH-6); 126.38 (CH-5); 124.75 (C-4a); 119.64 (CN); 119.52 (CH-3); 46.66 (CH-1''); 45.61 (CH₂-4''); 41.84 (CH₂-2'); 29.75 (CH₂-2''); 25.15 (CH₂-3'').

(S)-N-(2-(2-cyano-4,4-difluoropyrrolidin-1-yl)-2-oxoethyl)quinoline-4-carboxamide (R2)



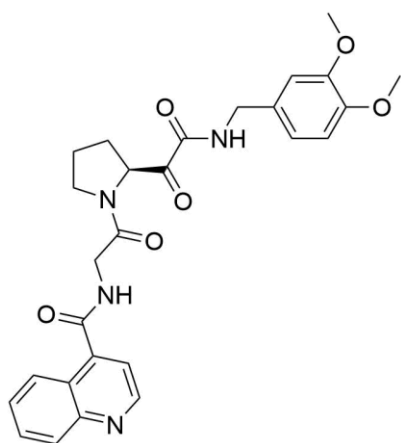
This compound was prepared according to a published procedure³.

UPLC/MS – $R_t = 3.258$ min, ESI+ $[M+H]^+ = 345.081$

¹H NMR (500 MHz, DMSO-*d*₆): 9.19 (bt, 1H, $J_{NH,2'} = 6.0$ Hz, NH-2'); 9.05 (d, 1H, $J_{2,3} = 4.4$ Hz, H-2); 8.38 (bdd, 1H, $J_{5,6} = 8.5$ Hz, $J_{5,7} = 1.5$ Hz, H-5); 8.12 (dm, 1H, $J_{8,7} = 8.5$ Hz, H-8); 7.87 (ddd, 1H, $J_{7,8} = 8.5$ Hz, $J_{8,7} = 6.9$ Hz, $J_{7,5} = 1.5$ Hz, H-7); 7.74 (ddd, 1H, $J_{6,5} = 8.5$ Hz, $J_{6,7} = 6.9$ Hz, $J_{6,8} = 1.3$ Hz, H-6); 7.64 (d, 1H, $J_{3,2} = 4.4$ Hz, H-3); 5.19 (dd, 1H, $J_{1'',2''} = 9.3$ and 2.6 Hz, H-1''); 4.34 (m, 1H, H-4''b); 4.28 (dd, 1H, $J_{gem} = 17.1$ Hz, $J_{2'b,NH} = 6.3$ Hz, H-2'b); 4.23 (dd, 1H, $J_{gem} = 17.1$ Hz, $J_{2'a,NH} = 5.7$ Hz, H-2'a); 4.15 (m, 1H, H-4''a); 3.01 - 2.78 (m, 2H, H-2'').

¹³C NMR (125.7 MHz, DMSO-*d*₆): 168.03 (CO-3'); 167.33 (CO-1'); 150.06 (CH-2); 147.08 (C-8a); 143.24 (C-4); 130.68 (CH-7); 128.67 (CH-8); 127.87 (CH-6); 127.21 (dd, $J_{C,F} = 250.4$ and 245.8 Hz, CH-3''); 126.10 (CH-5); 124.52 (C-4a); 119.36 (CH-3); 118.11 (CN); 51.40 (t, $J_{C,F} = 31.6$ Hz, CH₂-4''); 44.49 (d, $J_{C,F} = 6.4$ Hz, CH-1''); 41.58 (CH₂-2'); 36.60 (t, $J_{C,F} = 24.5$ Hz, CH₂-2'').

(S)-N-(2-(2-(2-((3,4-dimethoxybenzyl)amino)-2-oxoacetyl)pyrrolidin-1-yl)-2-oxoethyl)quinoline-4-carboxamide (R3)



UPLC/MS – $R_t = 3.13$ - 3.35 min, ESI+ $[M+H]^+ = 505.229$

¹H NMR (500 MHz, DMSO-*d*₆): 9.22 (bt, 1H, $J_{NH,CH_2} = 6.3$ Hz, COCONH); 9.03 – 8.97 (m, 2H, NH-2', H-2); 8.32 (dd, 1H, $J_{5,6} = 8.4$ Hz, $J_{5,7} = 1.4$ Hz, H-5); 8.09 (bd, 1H, $J_{8,7} = 8.5$ Hz, H-8); 7.83 (ddd, 1H, $J_{7,8} = 8.5$ Hz, $J_{8,7} = 6.9$ Hz, $J_{7,5} = 1.4$ Hz, H-7); 7.66 (ddd, 1H, $J_{6,5} = 8.5$ Hz, $J_{6,7} = 6.9$ Hz, $J_{6,8} = 1.2$ Hz, H-6); 7.57 (d, 1H, $J_{3,2} = 4.4$ Hz, H-3); 6.91 (d, 1H, $J_{2,6} = 2.0$ Hz, H-2-Ph); 6.86 (d, 1H, $J_{5,6} = 8.3$ Hz, H-5-Ph); 6.79 (dd, 1H, $J_{6,5} = 8.2$ Hz, $J_{6,2} = 2.0$ Hz, H-6-Ph); 5.23 (dd, 1H, $J_{1'',2''} = 9.2$ and 4.7 Hz, H-1''); 4.33 – 4.21 (m, 3H, CH₂-Ph, H-2'b); 4.15 (dd, 1H, $J_{gem} = 16.7$ Hz, $J_{2'a,NH} = 5.9$ Hz, H-2'a); 3.70 (s, 3H, CH₃O-3-Ph); 3.69 (s, 3H, CH₃O-4-Ph); 3.70 – 3.62 (m,

2H, H-4''); 2.24 (m, 1H, H-2''b); 2.01 (m, 1H, H-3''b); 1.90 (m, 1H, H-3''a); 1.84 (m, 1H, H-2''a).

¹³C NMR (125.7 MHz, DMSO-d₆): 195.66 (COCONH); 167.08 (CO-1'); 166.56 (CO-3'); 160.48 (COCONH); 150.15 (CH-2); 148.75 (C-3-Ph); 148.05 (C-4-Ph); 147.42 (C-8a); 142.98 (C-4); 131.10 (C-1-Ph); 130.40 (CH-7); 128.89 (CH-8); 127.69 (CH-6); 126.14 (CH-5); 124.49 (C-4a); 119.75 (CH-6-Ph); 119.33 (CH-3); 111.84 (CH-5-Ph); 111.69 (CH-2-Ph); 60.40 (CH-1'); 55.70 and 55.58 (CH₃O); 46.12 (CH₂-4'); 42.08 (CH₂-Ph); 41.54 (CH₂-2'); 27.95 (CH₂-2'); 24.81 (CH₂-3').

5.3 Measurement of Inhibitory Potencies

All IC₅₀ values were measured in a fluorogenic substrate assay, which was carried out according to a published protocol⁸⁵. The assay was performed on a microtiter plate, each well containing 0.5 ng of FAP in phosphate-buffered saline, containing 0.001% octaethylene glycol monododecyl ether. To this solution, an inhibitor solution was added to a total volume of 70 μ L. Ten different concentrations, obtained through serial dilution, were used. The reaction mixtures were pre-incubated for 5 minutes at 37 °C and then initiated by addition of the fluorogenic, FAP-specific substrate, *N*-(quinoline-4-carbonyl)-D-Ala-Pro-7-amino-4-methylcoumarin. The fluorescence of each well was recorded on an TECAN Infinite M1000 PRO fluorescence plate reader with a 380 nm excitation and 460 nm emission wavelength. Statistical interpretation of obtained data was performed in GraphPrism 8.3.1 software *via* non-linear regression. All IC₅₀ measurements were performed in duplicates.

Recombinant human DPPIV and recombinant human PREP were purchased from R&D Systems. Recombinant human FAP was prepared in the Konvalinka lab according to the formerly mentioned protocol.

6 References

1. W. J. Rettig, P. Garin-Chesa, H. R. Beresford, H. F. Oettgen, M. R. Melamed and L. J. Old, *Proc. Natl. Acad. Sci.*, **1988**, 85, 3110–3114.
2. P. Garin-Chesa, L. J. Old and W. J. Rettig, *Proc. Natl. Acad. Sci.*, **1990**, 87, 7235–7239.
3. K. Jansen, L. Heirbaut, R. Verkerk, J. D. Cheng, J. Joossens, P. Cos, L. Maes, A.-M. Lambeir, I. De Meester, K. Augustyns and P. Van der Veken, *J. Med. Chem.*, **2014**, 57, 3053–3074.
4. A. Aoyama and W.-T. Chen, *Proc Natl Acad Sci USA*, **1990**, 87, 8296–8300.
5. L. A. Goldstein, G. Gherzi, M. L. Piñeiro-Sánchez, Monica Salamone, Y. Yeh, D. Flessate and W.-T. Chen, *Biochim. Biophys. Acta - Mol. Basis Dis.*, **1997**, 1361, 11–19.
6. K. N. Lee, K. W. Jackson, V. J. Christiansen, K. H. Chung and P. A. McKee, *Blood*, **2004**, 103, 3783–3788.
7. K. N. Lee, K. W. Jackson, V. J. Christiansen, C. S. Lee, J.-G. Chun and P. A. McKee, *Blood*, **2006**, 107, 1397–1404.
8. J. Tillmanns, C. Widera, Y. Habbaba, P. Galuppo, T. Kempf, K. C. Wollert and J. Bauersachs, *Int. J. Cardiol.*, **2013**, 168, 3926–3931.
9. P. Busek, P. Hrabal, P. Fric and A. Sedo, *Histochem. Cell Biol.*, **2015**, 143, 497–504.
10. S. Bae, C. W. Park, H. K. Son, H. K. Ju, D. Paik, C.-J. Jeon, G. Y. Koh, J. Kim and H. Kim, *Br. J. Haematol.*, **2008**, 142, 827–830.
11. P. C. Schuberth, C. Hagedorn, S. M. Jensen, P. Gulati, M. van den Broek, A. Mischo, A. Soltermann, A. Jüngel, O. Marroquin Belaunzaran, R. Stahel, C. Renner and U. Petrusch, *J. Transl. Med.*, **2013**, 11, 187.
12. M. T. Levy, G. W. McCaughan, C. A. Abbott, J. E. Park, A. M. Cunningham, E. Müller, W. J. Rettig and M. D. Gorrell, *Hepatology. Baltim. Md*, **1999**, 29, 1768–1778.
13. M. T. Levy, G. W. McCaughan, G. Marinos and M. D. Gorrell, *Liver*, **2002**, 22, 93–101.
14. F. M. Keane, T.-W. Yao, S. Seelk, M. G. Gall, S. Chowdhury, S. E. Poplawski, J. H. Lai, Y. Li, W. Wu, P. Farrell, A. J. Vieira de Ribeiro, B. Osborne, D. M. T. Yu, D. Seth, K. Rahman, P. Haber, A. K. Topaloglu, C. Wang, S. Thomson, A. Hennessy, J. Prins, S. M. Twigg, S. V. McLennan, G. W. McCaughan, W. W. Bachovchin and M. D. Gorrell, *FEBS Open Bio*, **2013**, 4, 43–54.
15. P. S. Acharya, A. Zukas, V. Chandan, A.-L. A. Katzenstein and E. Puré, *Hum. Pathol.*, **2006**, 37, 352–360.

16. M. J. Scanlan, B. K. Raj, B. Calvo, P. Garin-Chesa, M. P. Sanz-Moncasi, J. H. Healey, L. J. Old and W. J. Rettig, *Proc. Natl. Acad. Sci. U. S. A.*, **1994**, 91, 5657–5661.
17. R. Bhati, C. Patterson, C. A. Livasy, C. Fan, D. Ketelsen, Z. Hu, E. Reynolds, C. Tanner, D. T. Moore, F. Gabrielli, C. M. Perou and N. Klauber-DeMore, *Am. J. Pathol.*, **2008**, 172, 1381–1390.
18. Y. Ge, F. Zhan, B. Barlogie, J. Epstein, J. Shaughnessy and S. Yaccoby, *Br. J. Haematol.*, **2006**, 133, 83–92.
19. K. Aertgeerts, I. Levin, L. Shi, G. P. Snell, A. Jennings, G. S. Prasad, Y. Zhang, M. L. Kraus, S. Salakian, V. Sridhar, R. Wijnands and M. G. Tennant, *J. Biol. Chem.*, **2005**, 280, 19441–19444.
20. N. D. Rawlings, A. J. Barrett, P. D. Thomas, X. Huang, A. Bateman and R. D. Finn, *Nucleic Acids Res.*, **2018**, 46, 624–632.
21. C. Klemann, L. Wagner, M. Stephan and S. von Hörsten, *Clin. Exp. Immunol.*, **2016**, 185, 1–21.
22. P. T. Männistö and J. A. García-Horsman, *Front. Aging Neurosci.*, **2017**, 9.
23. R. M. O’Leary, S. P. Gallagher and B. O’Connor, *Int. J. Biochem. Cell Biol.*, **1996**, 28, 441–449.
24. I. Schechter and A. Berger, *Biochem. Biophys. Res. Commun.*, **1967**, 27, 157–162.
25. C. Y. Edosada, C. Quan, C. Wiesmann, T. Tran, D. Sutherlin, M. Reynolds, J. M. Elliott, H. Raab, W. Fairbrother and B. B. Wolf, *J. Biol. Chem.*, **2006**, 281, 7437–7444.
26. S. E. Poplawski, J. H. Lai, Y. Li, Z. Jin, Y. Liu, W. Wu, Y. Wu, Y. Zhou, J. L. Sudmeier, D. G. Sanford and W. W. Bachovchin, *J. Med. Chem.*, **2013**, 56, 3467–3477.
27. M. Koida and R. Walter, *J. Biol. Chem.*, **1976**, 251, 7593–7599.
28. A. De Decker, G. Vliegen, D. Van Rompaey, A. Peeraer, A. Bracke, L. Verckist, K. Jansen, R. Geiss-Friedlander, K. Augustyns, H. De Winter, I. De Meester, A.-M. Lambeir and P. Van der Veken, *ACS Med. Chem. Lett.*, **2019**, 10, 1173–1179.
29. K. Jambunathan, D. S. Watson, A. N. Endsley, K. Kodukula and A. K. Galande, *FEBS Lett.*, **2012**, 586, 2507–2512.
30. L. Hedstrom, *Chem. Rev.*, **2002**, 102, 4501–4524.
31. R. Bone, A. B. Shenvi, C. A. Kettner and D. A. Agard, *Biochemistry*, **1987**, 26, 7609–7614.
32. T. L. Poulos, R. A. Alden, S. T. Freer, J. J. Birktoft and J. Kraut, *J. Biol. Chem.*, **1976**, 251, 1097–1103.
33. J. C. Powers, J. L. Asgian, Ö. D. Ekici and K. E. James, *Chem. Rev.*, **2002**, 102, 4639–4750.

34. M. Frizler, M. Stirnberg, M. Sisay and M. Gutschow, *Curr. Top. Med. Chem.*, **2010**, 10, 294–322.
35. T.-L. Ho, H. C. Ho and L. D. Hamilton, *Chem. Biol. Interact.*, **1978**, 23, 65–84.
36. I. Brandt, J. Joossens, X. Chen, M.-B. Maes, S. Scharpé, I. D. Meester and A.-M. Lambeir, *Biochem. Pharmacol.*, **2005**, 70, 134–143.
37. Y. B. Kim, L. M. Kopcho, M. S. Kirby, L. G. Hamann, C. A. Weigelt, W. J. Metzler and J. Marcinkeviciene, *Arch. Biochem. Biophys.*, **2006**, 445, 9–18.
38. W. J. Metzler, J. Yanchunas, C. Weigelt, K. Kish, H. E. Klei, D. Xie, Y. Zhang, M. Corbett, J. K. Tamura, B. He, L. G. Hamann, M. S. Kirby and J. Marcinkeviciene, *Protein Sci.*, **2008**, 17, 240–250.
39. A. El-Faham and F. Albericio, *Chem. Rev.*, **2011**, 111, 6557–6602.
40. I. Antonovics and G. T. Young, *J. Chem. Soc. C Org.*, **1967**, 595–601.
41. F. C. McKay and N. F. Albertson, *J. Am. Chem. Soc.*, **1957**, 79, 4686–4690.
42. T. T. Romoff and M. Goodman, *J. Pept. Res.*, **2009**, 49, 281–292.
43. L. A. Carpino, D. Ionescu and A. El-Faham, *J. Org. Chem.*, **1996**, 61, 2460–2465.
44. T. I. Al-Warhi, H. M. A. Al-Hazimi and A. El-Faham, *J. Saudi Chem. Soc.*, **2012**, 16, 97–116.
45. E. Valeur and M. Bradley, *Chem Soc Rev*, **2009**, 38, 606–631.
46. S.-Y. Han and Y.-A. Kim, *Tetrahedron*, **2004**, 60, 2447–2467.
47. J. C. Sheehan and G. P. Hess, *J. Am. Chem. Soc.*, **1955**, 77, 1067–1068.
48. W. König and R. Geiger, *Chem. Ber.*, **1970**, 103, 788–798.
49. L. A. Carpino and A. El-Faham, *Tetrahedron Lett.*, **1994**, 35, 2279–2282.
50. F. Albericio, J. M. Bofill, A. El-Faham and S. A. Kates, *J. Org. Chem.*, **1998**, 63, 9678–9683.
51. A. D. Fenza, M. Tancredi, C. Galoppini and P. Rovero, *Tetrahedron Lett.*, **1998**, 39, 8529–8532.
52. B. Trost, *Science*, **1991**, 254, 1471–1477.
53. C. Mannich and W. Krösche, *Arch. Pharm. (Weinheim)*, **1912**, 250, 647–667.
54. Passerini, M. and Simone, L., *Gazz. Chim. Ital.*, **1921**, 51, 126–129.
55. United States Patent and Trademark Office, US3247200A, **1966**.
56. P. L. Pauson and I. U. Khand, *Ann. N. Y. Acad. Sci.*, **1977**, 295, 2–14.
57. A. M. van Leusen, J. Wildeman and O. H. Oldenzie, *J. Org. Chem.*, **1977**, 42, 1153–1159.
58. K. Gewald, E. Schinke and H. Böttcher, *Chem. Ber.*, **1966**, 99, 94–100.
59. H. Staudinger, *Justus Liebigs Ann. Chem.*, **1907**, 356, 51–123.

60. L. Banfi, A. Basso, G. Guanti and R. Riva, *Mol. Divers.*, **2003**, 6, 227–235.
61. I. Ugi and C. Steinbrückner, *Chem. Ber.*, **1961**, 94, 734–742.
62. R. H. Baker and D. Stanonis, *J. Am. Chem. Soc.*, **1951**, 73, 699–702.
63. I. Ugi, *Angew. Chem. Int. Ed. Engl.*, **1962**, 1, 8–21.
64. L. Banfi, G. Guanti and R. Riva, *Chem. Commun.*, **2000**, 985–986.
65. L. Banfi, G. Guanti, R. Riva, A. Basso and E. Calcagno, *Tetrahedron Lett.*, **2002**, 3.
66. T. D. Owens and J. E. Semple, *Org. Lett.*, **2001**, 3, 3301–3304.
67. T. Ziegler and H.-J. Kaisers, *Tetrahedron*, **1999**, 55, 8397–8408.
68. C. L. Kelly, K. W. M. Lawrie, P. Morgan and C. L. Willis, *Tetrahedron Lett.*, **2000**, 41, 8001–8005.
69. T. D. Owens, G.-L. Araldi, R. F. Nutt and J. E. Semple, *Tetrahedron Lett.*, **2001**, 42, 6271–6274.
70. U. Schmidt and S. Weinbrenner, *J. Chem. Soc. Chem. Commun.*, **1994**, 1003.
71. Obrecht, R., Herrmann, R. and Ugi, I., *Synthesis*, **1985**, 400–402.
72. B. Y. Robert and B. Loren, *J. Am. Chem. Soc.*, **1948**, 70, 3721–3723.
73. R. Frey, S. G. Galbraith, S. Guelfi, C. Lamberth and M. Zeller, *Synlett*, **2003**, 1536–1538.
74. T. A. Keating and R. W. Armstrong, *J. Am. Chem. Soc.*, **1995**, 117, 7842–7843.
75. Y. Hu, L. Ma, M. Wu, M. S. Wong, B. Li, S. Corral, Z. Yu, T. Nomanbhoy, S. Alemayehu, S. R. Fuller, J. S. Rosenblum, N. Rozenkrants, L. C. Minimo, W. C. Ripka, A. K. Szardenings, J. W. Kozarich and K. R. Shreder, *Bioorg. Med. Chem. Lett.*, **2005**, 15, 4239–4242.
76. K. Narra, S. R. Mullins, H.-O. Lee, B. Strzemkowski-Brun, K. Magalong, V. J. Christiansen, P. A. McKee, B. Egleston, S. J. Cohen, L. M. Weiner, N. J. Meropol and J. D. Cheng, *Cancer Biol. Ther.*, **2007**, 6, 1691–1699.
77. C. Y. Edosada, C. Quan, T. Tran, V. Pham, C. Wiesmann, W. Fairbrother and B. B. Wolf, *FEBS Lett.*, **2006**, 580, 1581–1586.
78. S. A. Meadows, C. Y. Edosada, M. Mayeda, T. Tran, C. Quan, H. Raab, C. Wiesmann and B. B. Wolf, *Biochemistry*, **2007**, 46, 4598–4605.
79. T.-Y. Tsai, T. Hsu, C.-T. Chen, J.-H. Cheng, M.-C. Chiou, C.-H. Huang, Y.-J. Tseng, T.-K. Yeh, C.-Y. Huang, K.-C. Yeh, Y.-W. Huang, S.-H. Wu, M.-H. Wang, X. Chen, Y.-S. Chao and W.-T. Jiaang, *Bioorg. Med. Chem. Lett.*, **2009**, 19, 1908–1912.
80. K. Jansen, L. Heirbaut, J. D. Cheng, J. Joossens, O. Ryabtsova, P. Cos, L. Maes, A.-M. Lambeir, I. De Meester, K. Augustyns and P. Van der Veken, *ACS Med. Chem. Lett.*, **2013**, 4, 491–496.

81. G. Höfle, W. Steglich and H. Vorbrüggen, *Angew. Chem. Int. Ed. Engl.*, **1978**, 17, 569–583.
82. S. Xu, I. Held, B. Kempf, H. Mayr, W. Steglich and H. Zipse, *Chem. – Eur. J.*, **2005**, 11, 4751–4757.
83. E. Winterfeldt, *Synthesis*, 1975, 617–630.
84. J. D. More and N. S. Finney, *Org. Lett.*, **2002**, 4, 3001–3003.
85. P. Dvořáková, P. Bušek, T. Knedlík, J. Schimer, T. Etrych, L. Kostka, L. Stollinová Šromová, V. Šubr, P. Šácha, A. Šedo and J. Konvalinka, *J. Med. Chem.*, **2017**, 60, 8385–8393.